Design, Synthesis, and Biological Characterization of Bivalent 1-Methyl-1,2,5,6-tetrahydropyridyl-1,2,5-thiadiazole Derivatives as Selective Muscarinic Agonists

W. G. Rajeswaran,[†] Yang Cao,[‡] Xi-Ping Huang,[§] Mary Elizabeth Wroblewski,[‡] Tracy Colclough,[‡] Selina Lee,[‡] Fenghua Liu,[‡] Peter I. Nagy,[‡] James Ellis,[∥] Beth A. Levine,[∥] Karl H. Nocka,[∥] and William S. Messer, Jr.*[,‡]

Department of Medicinal and Biological Chemistry, Center for Drug Design and Development, College of Pharmacy, The University of Toledo, 2801 W. Bancroft Street, Toledo, Ohio 43606, Peptide Research Laboratory, SL12, Tulane University Health Sciences Center, 1430 Tulane Avenue, New Orleans, Louisiana 70012, SUNY Stony Brook, Stony Brook, New York, and UCB Research, Inc., 840 Memorial Drive, Cambridge, Massachusetts 02139

Received May 31, 2001

Selective muscarinic agonists could be useful in the treatment of neurological disorders such as Alzheimer's disease, schizophrenia, and chronic pain. Many muscarinic agonists have been developed, yet most exhibit at best limited functional selectivity for a given receptor subtype perhaps because of the high degree of sequence homology within the putative binding site, which appears to be buried within the transmembrane domains. Bivalent compounds containing essentially two agonist pharmacophores within the same molecule were synthesized and tested for receptor binding affinity and muscarinic agonist activity. A series of bis-1,2,5-thiadiazole derivatives of 1,2,5,6-tetrahydropyridine linked by an alkyloxy moiety exhibited very high affinity (K_i < 1 nM) and strong agonist activity. The degree of activity depended on the length of the linking alkyl group, which could be replaced by a poly(ethylene glycol) moiety, resulting in improved water solubility, binding affinity, and agonist potency.

Muscarinic receptors mediate a variety of physiological responses to the neurotransmitter acetylcholine in the central and peripheral nervous systems. Five subtypes of muscarinic receptor have been identified through molecular biological studies and characterized in various tissues using pharmacological techniques. The five muscarinic receptor subtypes have been classified as M_1−M_5, based on recommendations from the International Union of Pharmacology.[1] M_1 muscarinic receptors play a role in learning and memory function in the brain and regulate gastric acid secretion in the stomach. M_2 receptors regulate acetylcholine release in the central nervous system and control muscle contraction in the heart. Acetylcholine stimulates smooth muscle contraction in a variety of tissues and promotes secretion from exocrine glands. These effects are mediated by M_3 receptors. Though less well characterized pharmacologically, M_4 receptors appear to play a role in the perception of pain,[2] and M_5 receptors may regulate dopamine activity in the brain.

Despite the wealth of knowledge about muscarinic receptor subtypes, relatively few selective ligands are available to characterize muscarinic receptors. Efforts to develop selective compounds are hampered by the high degree of homology between receptor subtypes within the binding region of acetylcholine and other small molecules. Recent efforts have focused on developing larger muscarinic agonists that can interact with less highly conserved regions of the receptor.[3,4]

Sauerberg and colleagues developed a series of very potent muscarinic agonists based on the 1,2,5-thiadiazole group, which serves as an ester isostere.[5,6] A unique feature within this series of compounds is that extended alkyl groups can be accommodated while agonist activity is retained. We attempted to exploit this property of the 1,2,5-thiadiazole derivatives to synthesize and develop bivalent compounds containing essentially two agonist pharmacophores within the same molecule.

Bivalent ligands represent an important approach for medicinal chemists in the development of selective ligands. Previous studies have documented the successful application of the bivalent ligand approach in the development of selective κ-opioid antagonists such as norbinaltorphimine.[7,8]

A series of bivalent xanomeline derivatives was synthesized and examined for receptor binding and agonist activity at muscarinic receptor subtypes. The data indicate that the bivalent ligands exhibit markedly enhanced affinities and potencies compared to the parent compound xanomeline. Chemical manipulation of the linking group yielded compounds with improved solubility and potency. Moreover, a high degree of selectivity was apparent, suggesting the utility of designing molecules that can interact with multiple receptor domains.

Results and Discussion

Synthetic Chemistry. For the series with the alkyloxy linking groups (see Scheme 1), the starting material 3-(3-chloro-1,2,5-thiadiazol-4-yl)pyridine, **1**, was synthesized from 3-pyridinecarboxaldehyde using slight modifications of the published procedure.[5] Compound **1** was reacted with the appropriate diol **2a**−**j** in the

* To whom correspondence should be addressed. Phone: 419-530-1958. Fax: 419-530-7946. E-mail: wmesser@uoft02.utoledo.edu.
[†] Tulane University Health Sciences Center.
[‡] The University of Toledo.
[§] SUNY Stony Brook.
[∥] UCB Research, Inc.

10.1021/jm0102405 CCC: $20.00
Published on Web 11/15/2001

Scheme 1[a]

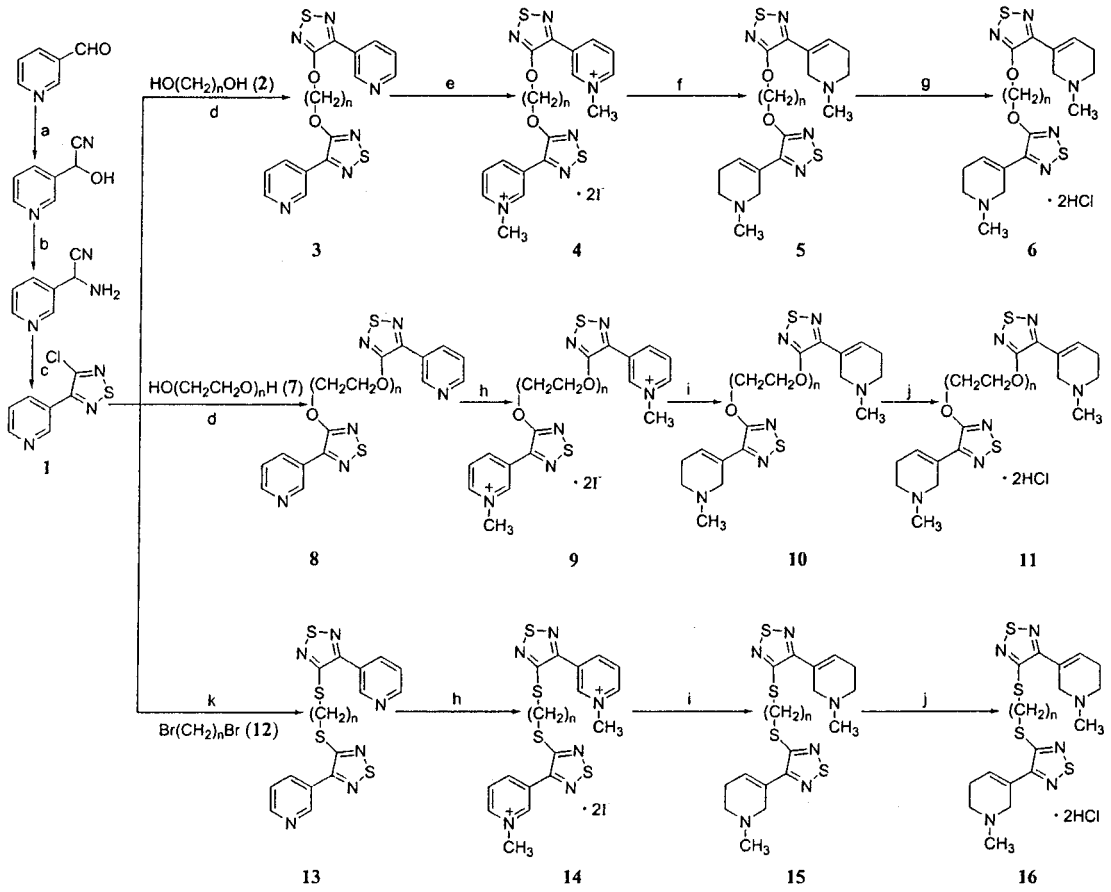

[a] Reagents: (a) KCN/H_2O/AcOH; (b) NH_4Cl/NH_3(aq); (c) S_2Cl_2/DMF; (d) NaH/THF; (e) MeI/acetone; (f) $NaBH_4$/MeOH; (g) MeOH/HCl, MeOH/ether; (h) MeI/acetone/CH_3Cl; (i) $NaBH_4$/MeOH/CH_3Cl; (j) MeOH/CH_3Cl/HCl, MeOH/ether, (k) NaSH·H_2O/DMF, K_2CO_3.

presence of sodium hydride in refluxing THF to yield bis[3-(pyrid-3-yl)-1,2,5-thiadiazol-4-yl]alkyl diethers (**3a**−**j**) in 75−90% yield. The diethers **3a**−**j** were treated with excess methyl iodide in acetone or chloroform to give the bis-quaternary ammonium iodides **4a**−**j** in 96−100% yield. After some experimentation, we found that the quaternary salts **4a**−**j** could be treated with 4 equiv of sodium borohydride in a mixture of methanol and chloroform to yield the tetrahydropyridyl derivatives, and the purified free bases (**5a**−**j**) were converted to the corresponding hydrochloride salts **6a**−**j** immediately by passing hydrogen chloride through their methanolic solution.

A separate series of compounds was synthesized using similar methods. The alkanediols were replaced with poly(ethylene glycols) (**7**) to form poly(ethylene glycol) di[3-(1-methyl-1,2,5,6-tetrahydropyrid-3-yl)-1,2,5-thiadiazol-4-yl] ether dihydrochlorides (**11a**−**e**) (see Scheme 1).

A third series of compounds containing thioether linkages was also synthesized (see Scheme 1). Briefly, sodium hydrogensulfide monohydrate was added to a solution of 3-(3-chloro-1,2,5-thiadiazol-4-yl)pyridine dissolved in THF and DMF. After addition of potassium carbonate, the appropriate amount of dibromoalkyl compound was reacted, followed by methylation and reduction to yield the desired bis[3-(1-methyl-1,2,5,6-tetrahydropyrid-3-yl)-1,2,5-thiadiazol-4-ylthio]alkane dihydrochlorides (**16a**−**k**).

Receptor Binding. Compounds were tested for receptor binding affinity and agonist activity in a variety of systems. Receptor binding affinity for human muscarinic receptor subtypes expressed in cell lines was assessed in competition assays using the labeled antagonist [^{3}H]-(*R*)-quinuclidinyl benzilate ([^{3}H]-(*R*)-QNB). At human M_1 receptors stably expressed in A9 L cells, the series of bivalent alkyloxy-1,2,5-thiadiazole derivatives of 1,2,5,6-tetrahydropyridine exhibited very high affinity, with K_i values typically less than 1 nM (see Table 1). The compound with the highest affinity was compound **6g**, with a K_i value of 0.19 nM. In comparison, xanomeline and carbachol had K_i values of 82 nM and 20 μM, respectively.

Compounds with a poly(ethylene glycol) linking group (e.g., **11c**) also exhibited high affinity for M_1 receptors (see Figure 1), with K_i values generally less than 10 nM (see Table 2). Compounds containing a thioether linking group also had high affinity for M_1 receptors (see Table 3).

Agonist Activity. Initial studies examined agonist activity for the bisthiadiazole derivatives at M_1 receptors coupled to phosphoinositide metabolism using a single concentration (100 μM) of test compounds. An interesting profile of agonist activity was observed, as shown in Table 1. Compounds with longer alkyloxy linkages, such as **6i** and **6j**, exhibited higher agonist activity, while moderate agonist activity also was observed with shorter alkyloxy groups (e.g., **6a**). In followup studies

Table 1. Receptor Binding Properties and Agonist Activity of Bisthiadiazole Ether Derivatives at M_1 Muscarinic Receptors Expressed in A9 L Cells[a]

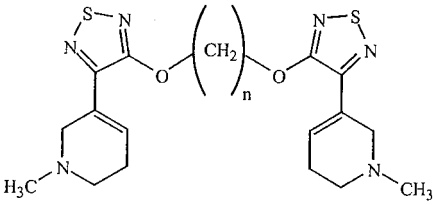

Compound	n
6a	2
6b	3
6c	4
6d	5
6e	6
6f	7
6g	8
6h	9
6i	10
6j	12

compound	K_i (nM)	PI metabolism (% at 100 μM)	EC_{50} (μM)	S_{max} (%)
carbachol	20000 ± 4100	100	13 ± 1.1	250 ± 15
xanomeline	82 ± 6.7	47 ± 5.3	0.057 ± 0.023	180 ± 24
6a	nd	50 ± 14	nd	nd
6b	nd	21 ± 2.6	nd	nd
6c	nd	21 ± 1.9	nd	nd
6d	nd	−1.0 ± 1.8	nd	nd
6e	0.61 ± 0.18	18 ± 0.06	nd	nd
6f	nd	−3.0 ± 3.4	nd	nd
6g	0.19 ± 0.004	8.2 ± 1.4	nd	nd
6h	0.84 ± 0.60	27 ± 6.2	0.72 ± 0.37	140 ± 34
6i	0.23 ± 0.10	76 ± 11	nd	nd
6j	1.6 ± 0.51	84 ± 9.9	0.34 ± 0.19	190 ± 61

[a] Binding data (K_i values) were obtained from competition assays utilizing [^{3}H]-(*R*)-QNB as the radioligand. PI metabolism represents the percentage stimulation above basal levels at 100 μM expressed relative to the carbachol response (100%). Full dose–response curves were obtained for **6h** and **6j** in the phosphoinositide metabolism assay. Data represent the mean (±SEM) from two to five assays for each compound. nd = not determined.

Table 2. Receptor Binding Properties and Agonist Activity of a Bisthiadiazole Polyethylene Glycol Derivative at M_1 Muscarinic Receptors Expressed in A9 L Cells[a]

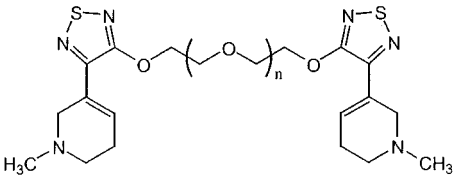

Compound	n
11a	1
11b	2
11c	3
11d	4
11e	5

compound	K_i (nM)	PI metabolism (% at 100 μM)	EC_{50} (μM)	S_{max} (%)
carbachol	20000 ± 4100	100	13 ± 1.1	250 ± 15
xanomeline	82 ± 6.7	47 ± 5.3	5.7 ± 2.3	180 ± 24
11a	4.9	<10	nd	nd
11b	nd	<10	nd	nd
11c	0.12 ± 0.057	56 ± 17	0.0085 ± 0.0012	250 ± 36
11d	1.5 ± 0.64	<10	nd	nd
11e	1.9 ± 0.91	<10	nd	nd

[a] Binding data (K_i values) were obtained from competition assays utilizing [^{3}H]-(*R*)-QNB as the radioligand. PI metabolism represents the percentage stimulation above basal levels at 100 μM expressed relative to the carbachol response (100%). Full dose–response curves were obtained for **11c** in the phosphoinositide metabolism assay. Data represent the mean (±SEM) from two to five assays for each compound. S_{max} values reflect the maximal level of stimulation as a percentage above basal levels. Data for carbachol and xanomeline are included for comparison. nd = not determined.

using a full range of concentrations, both **6h** and **6j** displayed lower potency than xanomeline and comparable agonist activity (S_{max}) at M_1 receptors expressed in A9 L cells.

Table 3. Receptor Binding Properties and Agonist Activity of Bisthiadiazole Thioether Derivatives at M_1 Muscarinic Receptors Expressed in A9 L Cells[a]

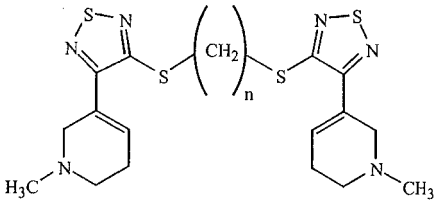

Compound	n
16a	2
16b	3
16c	4
16d	5
16e	6
16f	7
16g	8
16h	9
16i	10
16j	11
16k	12

compound	K_i (nM)	EC_{50} (μM)	S_{max} (%)
carbachol	20000 ± 4100	3.5 ± 0.35	780 ± 210
16a	20 ± 2.2	0.44 ± 0.090	300 ± 170
16b	1.2 ± 0.87	0.35 ± 0.20	250 ± 150
16c	0.93 ± 0.56	0.57 ± 0.004	510 ± 24
16d	14 ± 4.4	0.079 ± 0.023	880 ± 330
16e	0.87 ± 0.49	0.59 ± 0.24	770 ± 66
16f	7.6 ± 3.6	0.18 ± 0.075	830 ± 230
16g	5.0 ± 6.1	0.92	1300
16h	17 ± 6.2	0.12 ± 0.058	840 ± 110
16i	0.32 ± 0.12	2.1 ± 1.1	640 ± 430
16j	0.57 ± 0.15	1.5 ± 1.0	440 ± 9.1
16k	0.69 ± 0.31	13 ± 6.4	580 ± 250

[a] Binding data (K_i values) were calculated from competition assays utilizing [^{3}H]-(*R*)-QNB as the radioligand. S_{max} values reflect the maximal level of stimulation as a percentage above basal levels. Data represent the mean (±SEM) from two to five assays for each compound (except for **16g**). Note that expression levels of M_1 receptors were much higher than in studies outlined in Tables 1 and 2.

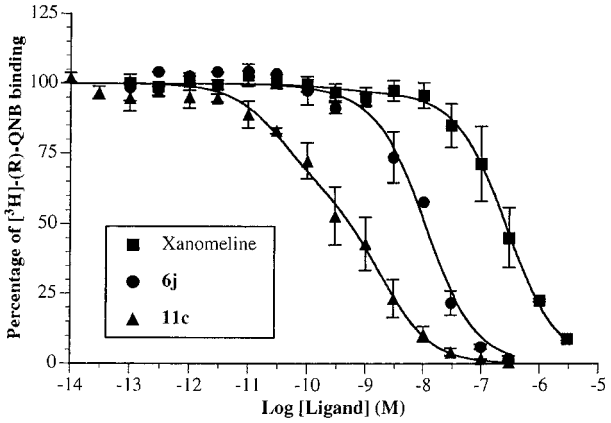

Figure 1. Inhibition of [^{3}H]-(*R*)-QNB binding to human M_1 receptors expressed in A9 L cells. Data represent the mean (±SEM) from three assays each performed in triplicate.

Similar results were obtained with the ethylene glycol derivatives, as shown in Table 2. Ligands with shorter linkages bound to receptors with high affinity but were inactive. One compound with a 13-atom linker (**11c**) bound with very high affinity and exhibited full agonist activity with remarkably high potency at M_1 receptors (see Figure 2).

In contrast to the compounds with alkyloxy linkages, all ligands within the thioalkyl series stimulated M_1 receptors expressed in A9 L cells (see Table 3). It should be noted that in the studies presented in Table 3, the expression level of M_1 receptors in A9 L cells was higher

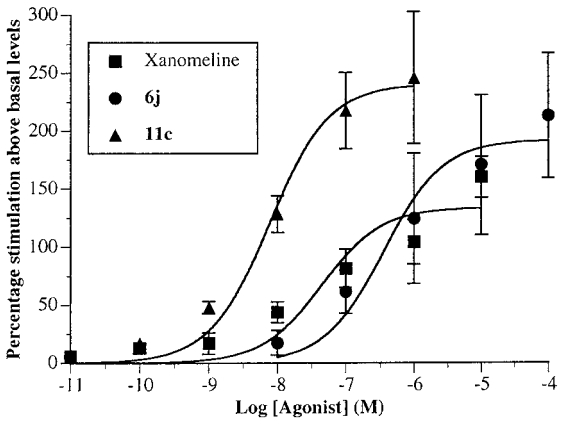

Figure 2. Stimulation of phosphoinositide metabolism in A9 L cells expressing human M_1 receptors. Data represent the mean (±SEM) from three assays each performed in duplicate and are fit to a one-site stimulation model.

Table 4. PI Hydrolysis Mediated by the Classical Muscarinic Agonists Acetylcholine and Carbachol at Human M_1 and M_5 Receptors Expressed in NIH 3T3 Cells[a]

	M_1 receptors		M_5 receptors	
ligand	EC_{50} (μM)	S_{max} (%)	EC_{50} (μM)	S_{max} (%)
acetylcholine	20 ± 5.5	550 ± 32	0.63 ± 0.11	99 ± 1.8
carbachol	130 ± 20	440 ± 29	8.9 ± 3.7	110 ± 8.0
xanomeline	2.6 ± 0.62	150 ± 1.2		7.9 ± 3.2
11c	0.29 ± 0.065	180 ± 18		−3.7 ± 4.5

[a] Data represent the mean (±SEM) from a minimum of three assays and are fit to a one-site stimulation model. S_{max} values reflect the maximal level of stimulation as a percentage above basal levels.

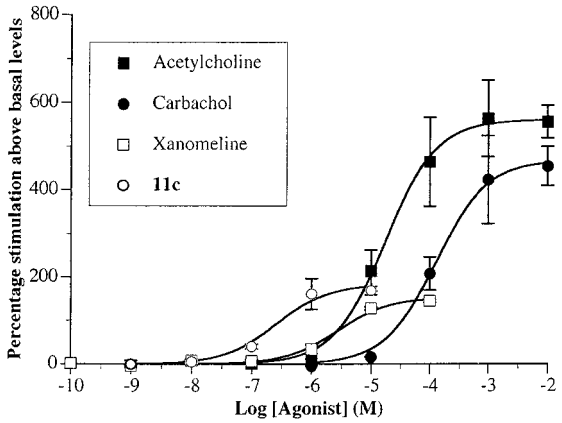

Figure 3. Stimulation of phosphoinositide metabolism in NIH 3T3 cells expressing human M_1 receptors. Data represent the mean (±SEM) from three assays each performed in duplicate and are fit to a one-site stimulation model.

than in the studies presented in Table 1. Thus, the relative activities of the thioalkyl derivatives cannot be compared directly with the compounds containing alkyloxy linking groups.

Both xanomeline and **11c** exhibited partial agonist activity at M_1 receptors expressed in NIH 3T3 cells (see Figure 3 and Table 4). Compound **11c** also was more potent than xanomeline, carbachol, and acetylcholine (Figure 3).

Functional Selectivity. Compounds displaying high agonist activity (e.g., **6j** and **11c**) were also examined for agonist activity at other muscarinic receptor subtypes. Both **6j** and **11c** were inactive at M_5 receptors expressed in NIH 3T3 cells (see Table 4). Xanomeline also was inactive at M_5 receptors.

Table 5. Agonist Activity of Bisthiadiazole Ether (**6**), Polyethylene Glycol (**11**), and Thioether (**16**) Derivatives at M_4 Muscarinic Receptors Expressed in RBL-2H3 Mast Cells[a]

compound	EC_{50} (nM)	maximal release (%)
carbachol	290 ± 57	87 ± 4.0
6a	3900	39
6e	>100000	3
6f	>100000	4
6g	>100000	1
6h	20000	61
6i	1100	24
6j	1.4	57
11c	5.2	43
16i	0.6	61
16j	4.7	29
16k	1.0	54

[a] Agonist activity was measured by the release of β-hexosaminidase and is a measure of degranulation. Percent release was calculated with a standard curve from 0% (unstimulated cells) to 100% release (cells lysed by 1% Triton-X100). The results were derived from single-point dose−response curves from 1 to 100 000 nM with 10-fold dilutions. The activity of the positive control carbachol is provided from four experiments as an indication of the reliability of this assay. The maximal release produced by the full agonist carbachol indicates the maximum possible response in this assay.

Table 6. Solubility Properties of Selected Compounds in Deionized Water and Kreb−Heinsleit Buffer (pH 7.4) at Room Temperature

compound	solubility in water	solubility in buffer
6i	25 mg/mL	4.0 μg/mL
6j	20 mg/mL	1.7 μg/mL
11c	>1 g/mL	20 μg/mL

The M_4 agonist activity of the bisthiadiazole ether derivatives was measured by their ability to induce degranulation of the rat RBL-2H3 mast cell clone that overexpresses the M_4 receptor (see Table 5). Compounds with the longest alkyloxy linkages such as **6j** had the greatest activities and potencies. Compound **6a**, with the shortest linkage, also had significant agonist activity. Compounds with intermediate linkers (i.e., **6e**−**g**) had no agonist activity at the M_4 receptor.

Compound **11c**, with the poly(ethylene glycol) linker of 13 atoms, also had strong M_4 agonist activity. Compounds **16i**, **16j**, and **16k** with the thioether linker of 12, 13, and 14 atoms, respectively, exhibited strong agonist activity at the M_4 receptor. Compound **16i** was the most potent and active compound of the series tested.

Solubility. Compounds with longer alkyl groups (i.e., **6i**, **6j**) had poor solubility in water and buffer (see Table 6). In addition, at high concentrations, agonist responses decreased dramatically as reflected by a decrease in the release of [^{3}H]-inositol phosphates (data not shown). Followup studies indicated that the decrease in the release of [^{3}H]-inositol phosphate was due to disruption of cell membranes during the incubation presumably because of the high lipid solubility of the alkyl linking group.

To improve water solubility, a series of ethylene glycol derivatives was synthesized. These compounds (e.g., **11c**) exhibited higher water solubility (see Table 6) and did not disrupt cell membranes (data not shown). Solubility in Kreb−Heinsleit buffer (pH 7.4) was also greater for **11c** compared with that for **6i** or **6j**.

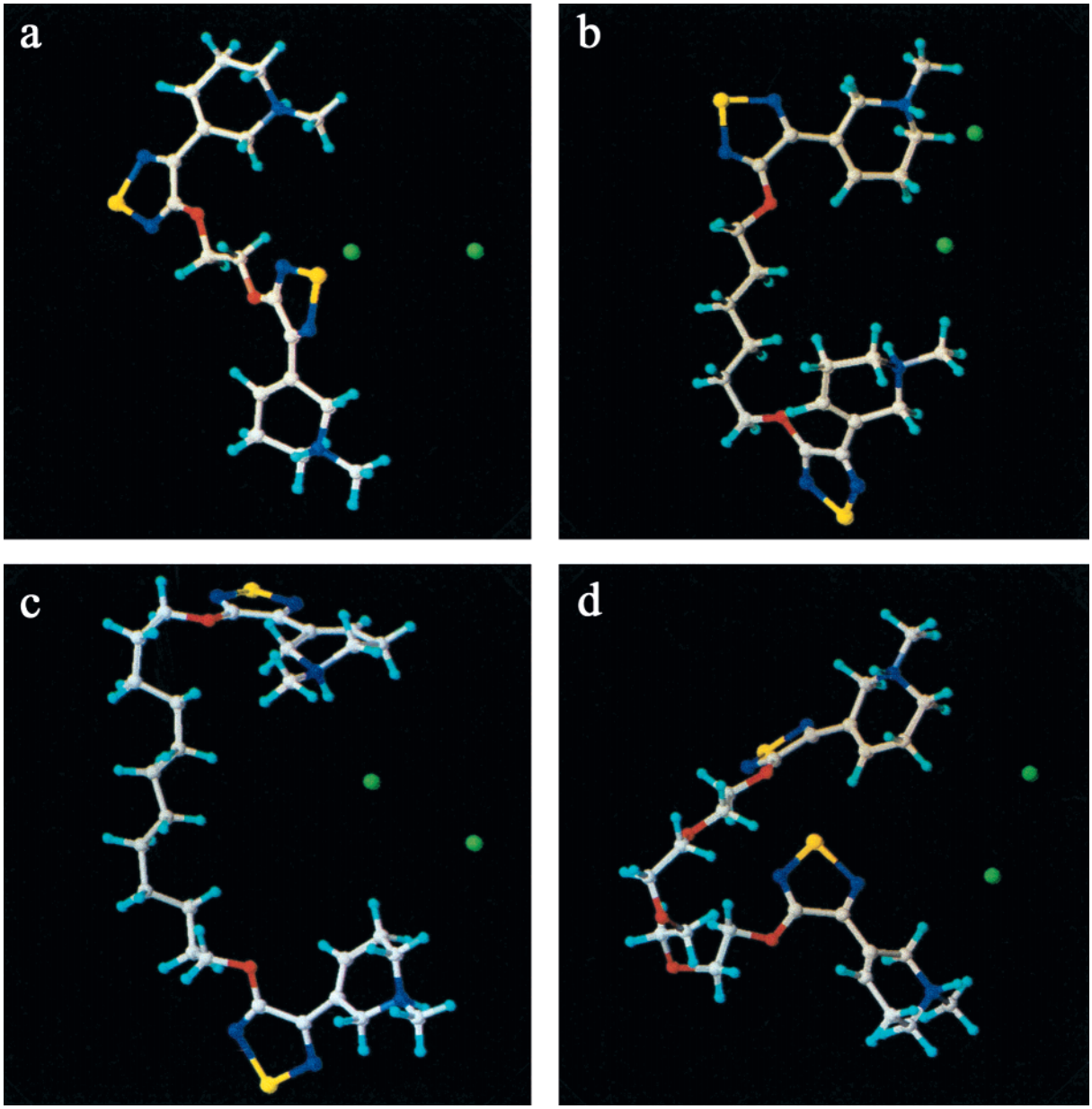

Figure 4. Conformation of **6a** (upper left), **6e** (upper right), **6j** (lower left), and **11c** (lower right) molecules at the end of molecular dynamics simulations in aqueous solution. Positions of the chloride counterions also are indicated. The color code is the following: C, white; H, cyan; N, blue; O, red; S, yellow; Cl, green.

Table 7. N···N Tertiary Amine Distances and Torsion Angles Calculated from Molecular Dynamics Simulations in Aqueous Solution[a]

	6a	**6e**	**6j**	**11c**
d(N···N), Å	9.79 ± 1.86	11.77 ± 0.82	10.54 ± 1.42, 10.37 ± 1.05	11.84 ± 1.41
d(max), Å	13.24	13.80	13.46, 12.90	15.49
d(min), Å	5.80	9.76	6.04, 7.37	8.04
torsion, %	65 (g)	20 (g)	27 (g), 36 (g)	47 (g)
			15 (−g), 18 (−g)	10 (−g)
	35 (t)	80 (t)	58 (t), 46 (t)	43 (t)

[a] Values *d*(max) and *d*(min) represent the maximum and minimum N···N distances, respectively, averaged in the last 200 ps of simulations. For the two sets for **6j**, see the text. The symbols g, t, and −g correspond to torsion angle ranges of 0−120°, 120−240°, and 240−360°, respectively.

Molecular Modeling. Molecular dynamics simulations for **6a**, **6e**, **6j**, and **11c** structures predicted fairly similar equilibrium N···N tertiary amine nitrogen distances with different molecular shapes (see Figure 4 and Table 7). The smallest average N···N distance was calculated for **6a**. The O−C−C−O torsion angle corresponded to a gauche arrangement for 65% of the calculations, but in the last 35% the torsion angle moved to trans, and this rodlike molecule produced an N···N distance as high as 13.24 Å. The average N···N distance was 11.77 ± 0.82 Å for **6e**. The O−$(CH_2)_6$−O linker had a fairly rigid structure; one O−C−C−C torsion angle was found as gauche, and the other four torsion angles along the linker kept their trans arrangement throughout the simulations. The large trans fraction resulted in relatively large average and *d*(max) values, and the

smallest standard deviation (SD) in the series reflected the torsional stability of the linker. The molecule adopted a horseshoe shape with, however, only a small curvature along the linker.

There are two sets of values for **6j** in Table 7. The first set was obtained as the average throughout a 200 ps simulation phase, where four NaCl molecules were added to the system (dication + 2Cl − counterion + 1235 TIP3P water molecules). The 4:1235 NaCl/water ratio nearly corresponds to the concentration of a physiological saline solution of 0.9 g of NaCl/100 cm^3. In the second set, data were obtained from the subsequent 100 ps simulations without the NaCl molecules. Comparison of the two sets of results revealed that consideration of the salt effect via NaCl molecules in the model system had nonsignificant effects on the average N···N distance. The fraction of the trans arrangement along the $O-(CH_2)_{12}-O$ linker was reduced by 12%, which may be important but may also indicate that even longer simulations are required for this ligand. (The total simulation time was 530 ps with the **6j** solute.)

In simulations for **6a**, only a single trans−gauche transformation was observed, and no conformational change was detected for **6e**. In contrast, there were a −g/t/−g double switch and two single switches, t/g and t/−g along the linker with the **6j** solute within its 200 ps averaging phase. Thus, the rigidity of the $-(CH_2)_n$ chain decreases with increasing *n*. Also, because of the 42−54% gauche conformation of the individual C−C−C−C moieties along the linker, the molecule adopts a butterfly or a horseshoe shape, which is much different from the molecular shape for **6a** and **6e** (see Figure 4).

Both the average and the maximum N···N distances were the largest for **11c** within the series. The linker is an ethylene glycol derivative with a structure of $O-CH_2-(CH_2-O-CH_2)_3-CH_2-O$. It is remarkable that the **11c** *d*(min) value was smaller than that for **6e** with only six $-CH_2-$ groups between the oxygens. This result can be primarily attributed to the flexibility of the −O− containing chain compared to the purely aliphatic linker. Indeed, a 1 ns gas-phase molecular dynamics simulation for **11c** showed repeated extensions of the molecule followed by conformations when the N···N distance decreased to a few angstroms. This result indicates the inherent flexibility of the linker in **11c**. The in-solution structure exhibited 57% local gauche arrangements, which is the largest in the calculated series. Furthermore, three −g/t and one t/−g single conformation switches were observed, and one double and one triple switches of the g/t/−g and −g/t/−g/t types were observed, respectively. All these together explain the large range of the N···N distances covered between *d*(min) and *d*(max). Not surprisingly, the structural analysis found **11c** to be the most flexible butterfly-shaped ligand of those studied.

The modeling studies provided several important insights. When approaching the receptor, the ligand is embedded in an aqueous environment with two counterions that were found to be stably located between the two cationic heads. The ligand either penetrates into the channel formed by the transmembrane helices and binds to the receptor in some cavity, or through some other hypothesized mechanism, it binds to some loop residues on the receptor surface. In the former case, a wormlike ligand can more easily penetrate into the channel. Here, the linker should be relatively short and should maintain a distance between the functional groups of the bivalent compound at some favorable value. It may be thermodynamically unfavorable for a ligand to take the worm shape, if having a long even flexible linker. In this case the ligand may bind to the receptor surface, and the in-solution equilibrium structure becomes important. Gradual dehydration and loss of the counterions should proceed in parallel with the binding process. A smaller activation energy is required if the in-solution structure can be easily accepted by the receptor throughout the ligand binding to two specific sites.

The PI metabolism data presented in Table 1 shows a minimum for the **6a**−**j** molecules. If assuming different mechanisms for **6a** and **6j**, the results of conformational studies can provide a rationale. While **6a** could penetrate into the channel formed by the transmembrane helices, **6j** (and also **11c**), having a long and flexible linker and a horseshoe or a butterfly shape, can favorably interact with residues of the third extracellular loop, for example. Using the newly developed, rhodopsin-based[9] M_1 receptor model, the $C_\alpha-C_\alpha$ distances were calculated at 12.1 and 15.7 Å for the Asp393−Glu397 and Asp393−Glu401 pairs, respectively, in the third extracellular loop.

Interaction of **6a** with the Asp393−Glu397 pair is unlikely. Although its in-solution N···N distance is not very far from the corresponding value for **11c** and the maximum N···N separation of 13.2 Å exceeds the calculated $C_\alpha\cdots C_\alpha$ distances of 12.1 Å, the lack of a flexible linker prevents **6a** from avoiding repulsive interactions with receptor atoms lying along the Asp−Glu $C_\gamma\cdots C_\delta$ axis in the third extracellular loop. Thus, a worm or rodlike molecule with a rigid linker generally cannot interact with fairly remote sites (except along an axis parallel with that of the transmembrane helix) because of the repulsion of the atoms lying along the (theoretical) axis connecting the sites. Many of these considerations may apply for **6e**, which is too large for favorably penetrating into the channel and has a linker that is too rigid for forming a favorable path between sites in the loop area. In conclusion, **6e** should be at least less active at either site where **6a**, **6j**, and **11c** are active, in accord with our experimental findings.

Site-directed mutagenesis[10−14] and molecular modeling studies[15,16] have identified several conserved residues that appear important for the binding of agonists to muscarinic receptors. Small-molecule agonists, such as acetylcholine and xanomeline, appear to interact with a primary binding site comprising key residues including Asp105,[10] Tyr381,[17] Thr192, and Asn382[18] for M_1 receptors. Recent site-directed mutagenesis studies have identified transmembrane domain (TM) VI and the third extracellular loop as regions important for switching muscarinic receptors between active and inactive conformations.[19−23]

In addition to the binding mode discussed above, flexible compounds such as **6j** and **11c** may interact with receptors in a manner such that one portion of the molecule binds to key residues buried within the transmembrane domain, while the second moiety is able to

Table 8. Calculated Energies for Docking of **11c** in the Muscarinic Receptor[a]

structure	E(RL)	E(R)	E(L)	$E(R_{opt})$	$E(L_{opt})$	E_{BE}	E_{IE}
I	−353	−351	31	−355	28	−26	−33
II	−366	−346	45	−355	28	−39	−65

[a] Energies are expressed in kcal/mol. E(RL): dimer energy. E(R): receptor energy in the dimer. E(L): ligand energy in the dimer. $E(R_{opt})$: optimized energy of the isolated receptor. $E(L_{opt})$: optimized energy of the isolated ligand. $E_{BE} = E(RL) - E(R_{opt}) - E(L_{opt})$. $E_{IE} = E(RL) - E(R) - E(L)$.

extend to the interface between TM VI and the third extracellular loop. This could place the second thiadiazole group in a position to interact with Ser388 and/or Thr389 at the interface of TM VI and the third extracellular loop. This hypothesis can be tested by examining the interaction of bivalent xanomeline derivatives with receptors in which Ser388 and Thr389 have been replaced. The penetration of such large molecules into the binding pocket requires a considerable opening of the channel that is, however, not seen on the available muscarinic receptor model based on rhodopsin.

For a computer-modeling validation of the above speculations, simple docking studies into our recent rhodopsin-based M_1 receptor model were performed for **11c**. Two conformations were considered for the ligand. In structure **I**, the MD output (see Figure 4d) was taken as the starting conformation, and after some small manual adjustments, the cationic heads were located in favorable positions for hydrogen bonding to the Asp393 and Glu397 carboxylate moieties. As mentioned above, the corresponding $C_\alpha - C_\alpha$ distance was calculated to be 12.1 Å from the model, thus being a favorable separation for a butterfly-shaped **11c** conformer. In structure **II**, the ligand was extended and placed into the channel surrounded by TM(III) and TM(VI). One cationic head of the bivalent ligand was placed close to the Asp105 carboxylate group while the other remained outside the transmembrane region, oriented toward the third extracellular loop (see Figure 5). Dimers **I** and **II** were optimized in a docking process using the Sybyl software.[24]

Computational results are summarized in Table 8. Because of the severe approximations applied (i.e., gas-phase dimerization, no solvent effects considered) the numerical values must be taken with caution. The relative values are more reasonable. Performing the calculations as previously,[18] the binding energy E_{BE} and the interaction energy E_{IE} (as defined in the footnote of Table 8) deserve attention. The dimer energy E(RL) is lower by 13 kcal/mol with structure **II** compared to the dimer energy of structure **I**. Thus, the contemporary binding of the stretched bivalent ligand at the hypothesized acetylcholine binding site of Asp105 and in the third extracellular loop is superior in comparison with a binding to two carboxylates in the third cellular loop. Although the calculated binding energies E_{BE} depend on the ill-defined optimized energy of the isolated receptor, R_{opt}, both values (−26 and −39 kcal/mol) are negative enough to suggest favorable binding in either of the two positions.

The difference in the interaction energies ΔE_{IE} is 32 kcal/mol (in favor of structure **II**) and is much larger than the 13 kcal/mol calculated for $\Delta E_{BE} = \Delta E$(RL). Inspection of the R and L terms reveals that E(R) and E(L) are less negative/more positive for structure **II** than for structure **I**. In fact the terms for structure **I** are only slightly higher than the corresponding optimized values. For structure **II**, $E(R) - E(R_{opt})$ and $E(L) - E(L_{opt})$ are as high as 9 and 17 kcal/mol, respectively. The results suggest that both components of the dimer undergo significant distortion in order to maximize the favorable interaction energy. A total distortion energy of 9 + 17 = 26 kcal/mol in the internal energy for the components of structure **II** results in −65 kcal/mol interaction energy. The corresponding values for structure **I** are 4 + 3 = 7 and −33 kcal/mol. Thus, it can be concluded that the bivalent ligand also favorably binds to the third extracellular loop, with a need for only a small geometric distortion. The binding and interaction energies are, however, superior when one of the cationic heads is bound in the acetylcholine binding cavity. This conformation of the ligand requires considerable extension of the linker moiety and is expected only with a very flexible linker. Figure 5b shows that the linker follows the available channel among the amino acid side chains. This flexibility is less expected for a more rigid $(CH_2)_n$ linker. Also, the $(CH_2-O-CH_2)_3$ linker makes possible a hydrogen bond to Ser388, which may be an important peculiarity of the binding and activity of **11c**.

The combination of synthetic medicinal chemistry, molecular modeling, site-directed mutagenesis, and receptor pharmacology provides useful information about the molecular details of accessory binding sites for muscarinic ligands. The concept of synthesizing ligands that interact with accessory binding sites for G-protein-coupled receptors has been helpful in the design of selective compounds. For example, Portoghese and colleagues recently identified a guanidinium derivative of naltrindol (GNTI) as a selective κ-antagonist.[25] GNTI was designed on the basis of modeling studies of the κ-antagonist norbinaltorphimine, suggesting that its two positively charged groups interacted with Asp138 in TM III and Glu297 at the top of TM VI. GNTI displayed high affinity for κ-receptors yet low affinity for μ-receptors. Mutation of Lys303 to Glu in μ-receptors dramatically enhanced the binding of GNTI, while mutation of Glu297 to Lys dramatically lowered the affinity of GNTI for κ-opioid receptors. It is interesting to note that Glu297 of κ-receptors and Lys303 of μ-receptors occupy a position similar to that of Ser388 in HM_1 receptors.

In summary, the series of bis-1,2,5-thiadiazole derivatives of 1,2,5,6-tetrahydropyridine exhibited very high affinity and strong agonist activity. The degree of activity depended on the length of the linking alkyl group, which could be replaced by a poly(ethylene glycol) moiety, resulting in improved water solubility, binding affinity, and agonist potency. Several compounds were identified with high activity and selectivity for M_1 and M_4 receptors. Further studies are necessary, however, to identify the molecular features necessary for high potency and activity to assess metabolic stability and to improve bioavailability and penetration into the central nervous system. Modification of the bivalent ligands ultimately could yield compounds with improved activity and selectivity for muscarinic receptor subtypes and could provide useful treatments for a variety of neurological disorders involving cholinergic systems,

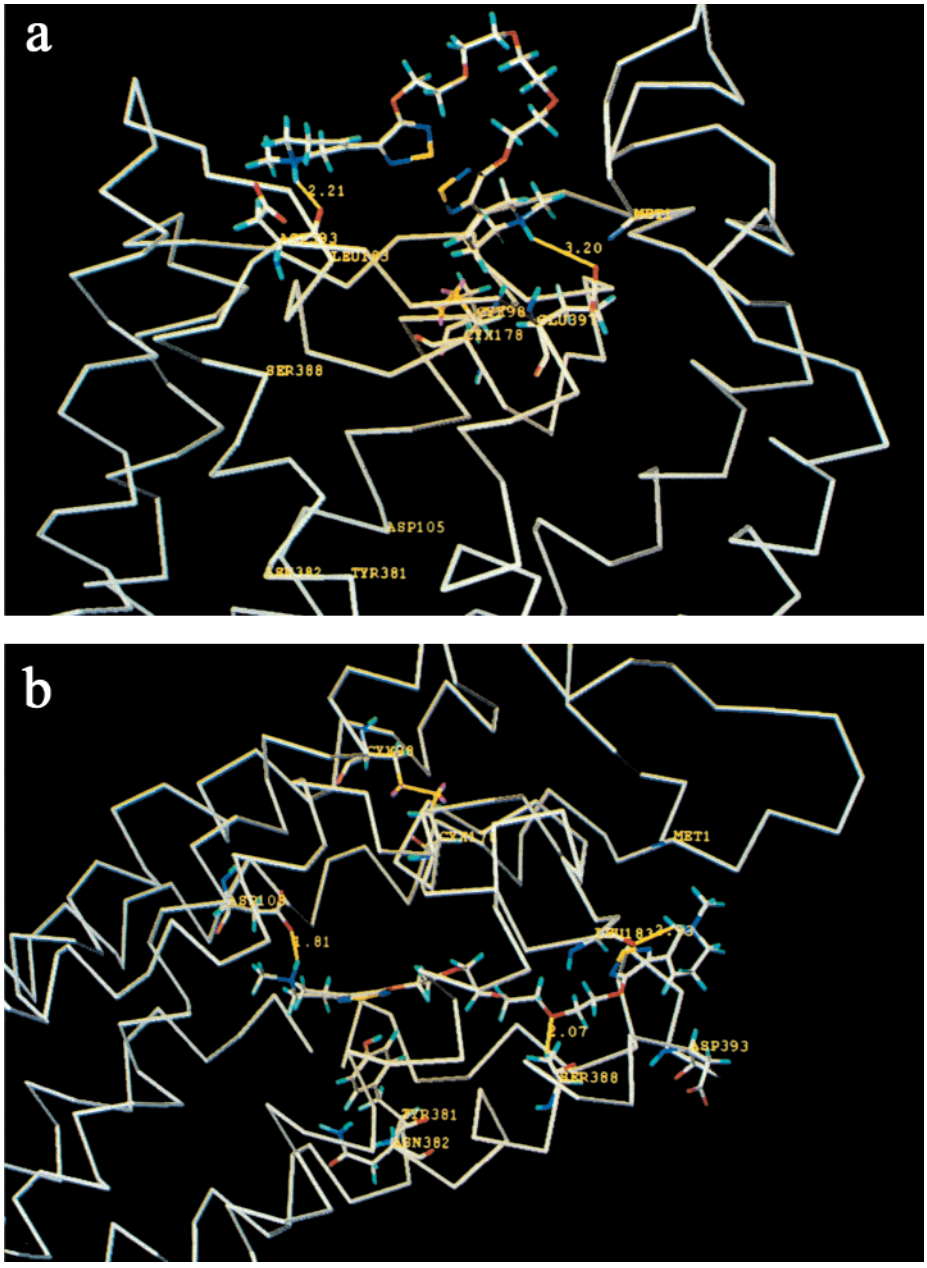

Figure 5. (a) Interaction of the horseshoe-shaped conformation of **11c** (structure **I**) with a model of the M_1 receptor depicting interactions with the third extracellular loop. Hydrogen bonds and short distances are marked by yellow lines: NH···O═C (Asp105) 2.21 Å; NH···OCO (Glu397) 3.20 Å. See also the disulfide bond between Cys98 and Cys178. (b) Interaction of an extended conformation of **11c** (structure **II**) with a model of the M_1 receptor highlighting interactions with the Asp105 residue in TM III and Ser388 at the junction of TM VI and the third extracellular loop. A near hydrogen bond distance is indicated between the unburied cationic group and the carbonyl oxygen of Leu183 in the second extracellular loop. Hydrogen bonds and short distances are marked by yellow lines: NH···OCO (Asp105) 1.81 Å; O···HO (Ser388) 2.01 Å; NH···O═C (Leu183) 2.93 Å. Note also the disulfide bond between Cys98 and Cys178. The color code is the following: C, white; H, cyan; N, blue; O, red; S, yellow.

including Alzheimer's disease, chronic pain, schizophrenia, and depression.

Experimental Section

Chemistry. Reactions were carried out under nitrogen. Melting points were determined on a Fisher-Johns melting point apparatus and are presented uncorrected. ^{1}H and ^{13}C NMR spectra were obtained with a Bruker ACF 300 MHz spectrometer. Elemental analyses (C, H, N) were performed by Atlantic Microlab, Inc., GA; the analytical results were within ±0.4% of the theoretical values for the formula given unless otherwise indicated. Precoated silica gel GHLF uniplates (250 μm) purchased from Analtech, Inc., DE, were used for TLC, and spots were examined with UV light at 254 nm or iodine vapor. Column chromatography purification was performed on Davisil silica gel 200−425 mesh obtained from Fisher Scientific. Tetrahydrofuran (THF) was dried over sodium benzophenone ketyl and distilled. All other commercially available solvents and reagents were used without further purfication unless otherwise specified.

General Procedure for the Preparation of Bis[3-(pyrid-3-yl)-1,2,5-thiadiazol-4-yloxy]alkanes (3). A suspension of 60% NaH in mineral oil (0.3 g, 7.5 mmol) was washed with hexane and suspended in THF (20 mL). To this suspension was added the appropriate diol compound (2.5 mmol), and the reaction mixture was stirred well for 15−30 min. Then a solution of 3-(3-chloro-1,2,5-thiadiazol-4-yl)pyridine (1.09 g, 5.5 mmol) in THF (15 mL) was added and the reaction mixture was refluxed for 20 h. The solvent was removed under reduced pressure, and ice-cold water was added

to the residue. The precipitated solid was filtered, washed with water, and dried. The dried crude compound was applied on a column of silica gel and eluted with the appropriate solvent mixture.

1,2-Bis[3-(pyrid-3-yl)-1,2,5-thiadiazol-4-yloxy]ethane (3a): yield 0.81 g (84%); mp 136−137 °C; ^{1}H NMR ($CDCl_3$) δ 5.0 (s, 4H), 7.35 (m, 2H), 8.4 (m, 2H), 8.65 (m, 2H), 9.4 (s, 2H). Anal. ($C_{16}H_{12}N_6O_2S_2$) C, H, N.

1,3-Bis[3-(pyrid-3-yl)-1,2,5-thiadiazol-4-yloxy]propane (3b): yield 0.76 g (76%); mp 103−104 °C; ^{1}H NMR ($CDCl_3$) δ 2.52 (m, 2H), 4.77 (t, 4H, J = 6.2 Hz), 7.35 (m, 2H), 8.37 (m, 2H), 8.65 (m, 2H), 9.36 (d, 2H, J = 2 Hz). Anal. ($C_{17}H_{14}N_6O_2S_2$) C, H, N.

1,4-Bis[3-(pyrid-3-yl)-1,2,5-thiadiazol-4-yloxy]butane (3c): yield 0.77 g (75%); mp 124−125 °C (EtOAc/hexane); ^{1}H NMR ($CDCl_3$) δ 2.15 (s, 4H), 4.65 (s, 4H, 2-OCH_2), 7.4 (m, 2H), 8.4 (m, 2H), 8.65 (m, 2H), 9.4 (s, 2H). Anal. ($C_{18}H_{16}N_6O_2S_2$) C, H, N.

1,5-Bis[3-(pyrid-3-yl)-1,2,5-thiadiazol-4-yloxy]pentane (3d): yield 0.95 g (89%); mp 97−98 °C (EtOAc/hexane); ^{1}H NMR ($CDCl_3$) δ 1.75 (m, 2H), 2.03 (m, 4H), 4.6 (t, 4H, J = 6.2 Hz, 2-OCH_2), 7.4 (m, 2H), 8.4 (m, 2H), 8.65 (s, 2H), 9.4 (s, 2H). Anal. ($C_{19}H_{18}N_6O_2S_2$) C, H, N.

1,6-Bis[3-(pyrid-3-yl)-1,2,5-thiadiazol-4-yloxy]hexane (3e): yield 0.94 g (86%); mp 114−115 °C (EtOAc/hexane); ^{1}H NMR ($CDCl_3$) δ 1.5−1.65 (m, 4H), 1.9−2.05 (m, 4H), 4.55 (t, 4H, 2-OCH_2), 7.3−7.4 (m, 2H), 8.35−8.45 (m, 2H), 8.62−8.66 (m, 2H), 9.39 (d, 2H). Anal. ($C_{20}H_{20}N_6O_2S_2$) C, H, N.

1,7-Bis[3-(pyrid-3-yl)-1,2,5-thiadiazol-4-yloxy]heptane (3f): yield 0.98 g (86%); mp 79 °C (EtOAc/hexane); ^{1}H NMR ($CDCl_3$) δ 1.45−1.6 (m, 6H), 1.9 (m, 4H), 4.53 (t, 4H, J = 6.8 Hz), 7.39 (m, 2H), 8.42 (m, 2H), 8.64 (dd, 2H, J = 1.6 and 4.8 Hz), 9.4 (s, 2H). Anal. ($C_{21}H_{22}N_6O_2S_2$) C, H, N.

1,8-Bis[3-(pyrid-3-yl)-1,2,5-thiadiazol-4-yloxy]octane (3g): yield 0.95 g (81%); mp 115−116 °C (EtOAc/hexane); ^{1}H NMR ($CDCl_3$) δ 1.4 (m, 8H), 1.89 (m, 4H), 4.52 (t, 4H, J = 6.4 Hz), 7.37 (m, 2H), 8.41 (m, 2H), 8.63 (m, 2H), 9.39 (d, 2H, J = 1.6 Hz). Anal. ($C_{22}H_{24}N_6O_2S_2$) C, H, N.

1,9-Bis[3-(pyrid-3-yl)-1,2,5-thiadiazol-4-yloxy]nonane (3h): yield 1.06 g (88%); mp 61 °C (EtOAc/hexane); ^{1}H NMR ($CDCl_3$) δ 1.4−1.55 (m, 10H), 1.8−1.9 (m, 4H), 4.5 (t, 4H, 2-OCH_2), 7.4 (m, 2H), 8.45 (d, 2H), 8.65 (d, 2H), 9.4 (s, 2H). Anal. ($C_{23}H_{26}N_6O_2S_2$) C, H, N.

1,10-Bis[3-(pyrid-3-yl)-1,2,5-thiadiazol-4-yloxy]decane (3i): yield 1.02 g (82%); mp 95 °C (EtOAc/hexane); ^{1}H NMR ($CDCl_3$) δ 1.3−1.6 (m, 12H), 1.9 (m, 4H), 4.55 (t, 4H, 2-OCH_2), 7.4 (m, 2H), 8.45 (m, 2H), 8.65 (m, 2H), 9.4 (d, 2H). Anal. ($C_{24}H_{28}N_6O_2S_2$) C, H, N.

1,12-Bis[3-(pyrid-3-yl)-1,2,5-thiadiazol-4-yloxy]dodecane (3j): yield 1.03 g (79%); mp 79 °C (EtOAc/hexane); ^{1}H NMR ($CDCl_3$) δ 1.3−1.55 (m, 16H), 1.85−2.0 (m, 4H), 4.5 (t, 4H, 2-OCH_s), 7.4 (m, 2H), 8.4 (m, 2H), 8.65 (m, 2H), 9.4 (d, 2H). Anal. ($C_{26}H_{32}N_6O_2S_2$) C, H, N.

General Procedure for the Preparation of Quaternary Salts of Bis[3-(pyrid-3-yl)-1,2,5-thiadiazol-4-yloxy]alkanes (4). To a solution of an appropriate compound **3** (1 mmol) in acetone (25 mL) was added excess MeI (3 mL, 48 mmol), and the solution was stirred for 36 h at room temperature. The precipitated was filtered, washed with acetone, and dried.

1,2-Bis[3-(1-methylpyridinium-3-yl)-1,2,5-thiadiazol-4-yloxy]ethane diiodide (4a): yield 0.66 g (99%); mp 200−202 °C; ^{1}H NMR (DMSO) δ 4.44 (s, 6H, N−Me), 5.08 (s, 4H), 8.22 (m, 2H), 9.07 (m, 4H), 9.55 (s, 2H).

1,3-Bis[3-(1-methylpyridinium-3-yl)-1,2,5-thiadiazol-4-yloxy]propane diiodide (4b): yield 0.68 g (100%); mp 128−130 °C; ^{1}H NMR (DMSO) δ 2.1 (s, 4H), 4.45 (s, 6H, N−Me), 4.65 (s, 4H), 8.3 (m, 2H), 9.1 (m, 4H), 9.5 (s, 2H). Anal. ($C_{19}H_{20}N_6O_2S_2I_2$) C, H, N.

1,4-Bis[3-(1-methylpyridinium-3-yl)-1,2,5-thiadiazol-4-yloxy]butane diiodide (4c): yield 0.7 g (100%); ^{1}H NMR (DMSO) δ 2.1 (s, 4H), 4.45 (s, 6H, N−Me), 4.65 (s, 4H), 8.3 (m, 2H), 9.1 (m, 4H), 9.5 (s, 2H).

1,5-Bis[3-(1-methylpyridinium-3-yl)-1,2,5-thiadiazol-4-yloxy]pentane diiodide (4d): yield 0.67 g (94%); mp 167−169 °C (dec); ^{1}H NMR (DMSO) δ 1.65 (m, 2H), 2.0 (m, 4H), 4.45 (s, 6H, N−Me), 4.6 (t, 4H, J = 6.8 Hz), 8.3 (m, 2H), 9.05 (m, 4H), 9.5 (s, 2H). Anal. ($C_{21}H_{24}N_6O_2S_2I_2$) C, H, N.

1,6-Bis[3-(1-methylpyridinium-3-yl)-1,2,5-thiadiazol-4-yloxy]hexane diiodide (4e): yield 0.7 g (97%); mp 194−196 °C (dec); ^{1}H NMR (DMSO) δ 1.55 (m, 4H), 1.92 (m, 4H), 4.45 (s, 6H, N−Me), 4.57 (t, 4H, J = 6.8 Hz), 8.3 (m, 2H), 9.15 (m, 4H), 9.5 (s, 2H). Anal. ($C_{22}H_{26}N_6O_2S_2I_2$) C, H, N.

1,7-Bis[3-(1-methylpyridinium-3-yl)-1,2,5-thiadiazol-4-yloxy]heptane diiodide (4f): yield 0.74 g (100%); ^{1}H NMR (DMSO) δ 1.5 (m, 6H), 1.9 (m, 4H), 4.45 (s, 6H, N−Me), 4.55 (t, 4H, J = 6.8 Hz), 8.3 (m, 2H), 9.05 (m, 4H), 9.5 (s, 2H).

1,8-Bis[3-(1-methylpyridinium-3-yl)-1,2,5-thiadiazol-4-yloxy]octane diiodide (4g): yield 0.71 g (94%); mp 150−152 °C (dec); ^{1}H NMR (DMSO) δ 1.35−1.55 (m, 8H), 1.9 (m, 4H), 4.5 (s, 6H), 4.55 (t, 4H, J = 6.8 Hz), 8.34 (m, 2H), 9.1 (m, 4H), 9.55 (s, 2H). Anal. ($C_{24}H_{30}N_6O_2S_2I_2$) C, H, N.

1,9-Bis[3-(1-methylpyridinium-3-yl)-1,2,5-thiadiazol-4-yloxy]nonane diiodide (4h): yield 0.74 g (97%); mp 163−165 °C; ^{1}H NMR (DMSO) δ 1.35−1.5 (m, 10H), 1.85 (m, 4H), 4.46 (s, 6H, N−Me), 4.54 (t, 4H, J = 6.8 Hz), 8.29 (m, 2H), 9.07 (m, 4H), 9.51 (s, 2H). Anal. ($C_{25}H_{32}N_6O_2S_2I_2$) C, H, N.

1,10-Bis[3-(1-methylpyridinium-3-yl)-1,2,5-thiadiazol-4-yloxy]decane diiodide (4i): yield 0.77 g (99%); mp 136−138 °C; ^{1}H NMR (DMSO) δ 1.3−1.5 (m, 12H), 1.9 (m, 4H), 4.47 (s, 6H, N−Me), 4.55 (t, 4H, J = 6.8 Hz), 8.3 (m, 2H), 9.1 (m, 4H), 9.5 (s, 2H). Anal. ($C_{26}H_{34}N_6O_2S_2I_2$) C, H, N.

1,12-Bis[3-(1-methylpyridinium-3-yl)-1,2,5-thiadiazol-4-yloxy]dodecane diiodide (4j): yield 0.81 g (100%); mp 119−122 °C (dec); ^{1}H NMR (DMSO) δ 1.2−1.5 (m, 16H), 1.9 (m, 4H), 4.45 (s, 6H, N−Me), 4.55 (t, 4H, J = 6.8 Hz), 8.3 (m, 2H), 9.1 (m, 4H), 9.5 (s, 2H). Anal. ($C_{28}H_{38}N_6O_2S_2I_2$) C, H, N.

General Procedure for the Preparation of Bis[3-(1-methyl-1,2,5,6-tetrahydropyrid-3-yl)-1,2,5-thiadiazol-4-yloxy]alkane Dihydrochlorides (6). Compound **4** (0.5 mmol) was dissolved in a mixture of $CHCl_3$ (10 mL) and MeOH (10 mL). The solution was cooled to 0−5 °C, and $NaBH_4$ (0.08 g, 2 mmol) was added to the reaction mixture. It was stirred at 0−5 °C for 2 h. Then cold H_2O and more $CHCl_3$ (30 mL) were added to the reaction mixture and the organic layer was separated and dried. The solvent was removed under reduced pressure, and the residue was chromatographed on a column of silica gel (eluent 1:10 MeOH/EtOAc). The purified compound was dissolved in MeOH (10 mL), and the solution was cooled to 0 °C. Then dry HCl was bubbled through the solution for 3 min and cold ether was added to precipitate the dihydrochloride salt. The precipitated solid was filtered, washed with ether, and dried.

1,2-Bis[3-(1-methyl-1,2,5,6-tetrahydropyrid-3-yl)-1,2,5-thiadiazol-4-yloxy]ethane dihydrochloride (CDD-0268-A) (6a): yield 0.14 g (56%); mp 217−218 °C; ^{1}H NMR (D_2O) δ 2.5 (m, 4H), 2.89 (s, 6H, N−Me), 3.1 (m, 2H), 3.48 (m, 2H), 3.88 (m, 2H), 4.31 (m, 2H), 4.84 (s, 4H, 2-OCH_2), 6.98 (m, 2H, vinylic). Anal. ($C_{18}H_{24}N_6O_2S_2\cdot 2HCl\cdot H_2O$) C, H, N.

1,3-Bis[3-(1-methyl-1,2,5,6-tetrahydropyrid-3-yl)-1,2,5-thiadiazol-4-yloxy]propane dihydrochloride (CDD-0267-A) (6b): yield 0.13 g (52%); mp 219−220 °C; ^{1}H NMR (D_2O) δ 2.27 (m, 2H), 2.49 (m, 4H), 2.87 (s, 6H, N−Me), 3.1 (m, 2H), 3.45 (m, 2H), 3.82 (m, 2H), 4.27 (m, 2H), 4.52−4.64 (m, 6H), 6.95 (m, 2H, vinylic). Anal. ($C_{19}H_{26}N_6O_2S_2\cdot 2HCl\cdot H_2O$) C, H, N.

1,4-Bis[3-(1-methyl-1,2,5,6-tetrahydropyrid-3-yl)-1,2,5-thiadiazol-4-yloxy]butane dihydrochloride (CDD-0266-A) (6c): yield 0.13 g (50%); ^{1}H NMR (D_2O) δ 1.9 (m, 4H), 2.4−2.65 (m, 4H), 2.85 (s, 6H, N−Me), 3.0−3.1 (m, 2H), 3.4−3.5 (m, 2H), 3.6−3.8 (m, 2H), 4.15−4.25 (m, 2H), 4.35−4.5 (m, 4H), 6.95 (m, 2H). Anal. ($C_{20}H_{28}N_6O_2S_2\cdot 2HCl\cdot 2.5H_2O$) C, H, N.

1,5-Bis[3-(1-methyl-1,2,5,6-tetrahydropyrid-3-yl)-1,2,5-thiadiazol-4-yloxy]pentane dihydrochloride (CDD-0265-A) (6d): yield 0.16 g (60%); mp 175−177 °C; ^{1}H NMR (D_2O) δ 1.4−1.5 m, 2H), 1.7−1.8 (m, 4H), 2.4−2.65 (m, 4H), 2.85 (s,

6H, N−Me), 3.1 (m, 2H), 3.45 (m, 2H), 3.7 (m, 2H), 4.2−4.4 (m, 6H), 7.02 (m, 2H). Anal. ($C_{21}H_{30}N_6O_2S_2$·2HCl·H_2O) C, H, N.

1,6-Bis[3-(1-methyl-1,2,5,6-tetrahydropyrid-3-yl)-1,2,5-thiadiazol-4-yloxy]hexane dihydrochloride (CDD-0257-A) (6e): yield 0.18 g (67%); ^{1}H NMR (D_2O) δ 1.35 (m, 4H), 1.7 (m, 4H), 2.5 (m, 4H), 2.87 (s, 6H, N−Me), 3.1 (m, 2H), 3.4 (m, 2H), 3.85 (m, 2H), 4.3 (m, 6H), 7.02 (m, 2H). Anal. ($C_{22}H_{32}N_6O_2S_2$·2HCl·0.5H_2O) C, H, N.

1,7-Bis[3-(1-methyl-1,2,5,6-tetrahydropyrid-3-yl)-1,2,5-thiadiazol-4-yloxy]heptane Dihydrochloride (CDD-0263-A) (6f): yield 0.14 g (50%); mp 179−181 °C; ^{1}H NMR (D_2O) δ 1.25−1.4 (m, 6H), 1.7 (m, 4H), 2.45−2.65 (m, 4H), 2.9 (s, 6H, N−Me), 3.1 (m, 2H), 3.45 (m, 2H), 3.85 (m, 2H), 4.3 (m, 6H), 7.05 (m, 2H). Anal. ($C_{23}H_{34}N_6O_2S_2$·2HCl·0.5H_2O) C, H, N.

1,8-Bis[3-(1-methyl-1,2,5,6-tetrahydropyrid-3-yl)-1,2,5-thiadiazol-4-yloxy]octane dihydrochloride (CDD-0260-A) (6g): yield 0.17 g (59%); mp 172−174 °C; ^{1}H NMR (D_2O) δ 1.25 (m, 8H), 1.66 (m, 4H), 2.58 (m, 4H), 2.88 (s, 6H, N−Me), 3.11 (m, 2H), 3.46 (m, 2H), 3.84 (m, 2H), 4.29 (m, 6H), 7.08 (m, 2H, vinylic). Anal. ($C_{24}H_{36}N_6O_2S_2$·2HCl) C, H, N.

1,9-Bis[3-(1-methyl-1,2,5,6-tetrahydropyrid-3-yl)-1,2,5-thiadiazol-4-yloxy]nonane dihydrochloride (CDD-0262-A) (6h): yield 0.05 g (17%); mp 156−158 °C; ^{1}H NMR (D_2O) δ 1.1−1.35 (m, 10H), 1.55−1.7 (m, 4H), 2.45−2.65 (m, 4H), 2.85 (s, 6H, N−Me), 3.05−3.15 (m, 2H), 3.4−3.5 (m, 2H), 3.85 (m, 2H), 4.3 (m, 6H), 7.05 (m, 2H, vinylic). Anal. ($C_{25}H_{38}N_6O_2S_2$·2HCl·1.5H_2O) C, H, N.

1,10-Bis[3-(1-methyl-1,2,5,6-tetrahydropyrid-3-yl)-1,2,5-thiadiazol-4-yloxy]decane dihydrochloride (CDD-0261-A) (6i): yield 0.14 g (46%); ^{1}H NMR (D_2O) δ 1.05−1.3 (m, 12H), 1.6−1.7 (m, 4H), 2.5−2.7 (m, 4H), 2.85 (s, 6H, N−Me), 3.1 (m, 2H), 3.4−3.5 (m, 2H), 3.85 (m, 2H), 4.3 (m, 6H), 7.05 (m, 2H, vinylic). Anal. ($C_{26}H_{40}N_6O_2S_2$·2HCl·0.5H_2O) C, H, N.

1,12-Bis[3-(1-methyl-1,2,5,6-tetrahydropyrid-3-yl)-1,2,5-thiadiazol-4-yloxy]dodecane dihydrochloride (CDD-0264-A) (6j): yield 0.18 g (56%); mp 155−157 °C; ^{1}H NMR (D_2O) δ 0.95−1.3 (m, 16H), 1.6 (m, 4H), 2.4−2.65 (m, 4H), 2.85 (s, 6H, N−Me), 3.05 (m, 2H), 3.45 (m, 2H), 3.8 (m, 2H), 4.1−4.3 (m, 6H), 6.95 (m, 2H, vinylic). Anal. ($C_{28}H_{42}N_6O_2S_2$·2HCl·H_2O) C, H, N.

General Procedure for the Preparation of Poly(ethylene glycol) Di[3-(pyrid-3-yl)-1,2,5-thiadiazol-4-yl] Ethers (8). A suspension of 60% NaH in mineral oil (200 mg, 5 mmol) was washed with anhydrous hexane (10 mL) and suspended in freshly distilled THF (20 mL). Then poly(ethylene glycol) (1 mmol) was added to the above suspension and the reaction mixture was refluxed for 1 h. 3-(3-Chloro-1,2,5-thiadiazol-4-yl)pyridine (500 mg, 2.53 mmol) in THF (15 mL) was added, and the reaction mixture was refluxed for 24 h. The mixture was evaporated under a vacuum and quenched with ice−water (20 mL), then the aqueous solution was extracted with $CHCl_3$ twice. The combined extract was washed with water, dried over anhydrous Na_2SO_4, and concentrated to yield the crude compounds.

Di(ethylene glycol) Di[3-(pyrid-3-yl)-1,2,5-thiadiazol-4-yl] Ether (8a). The crude pale-yellow powder was purified by silica gel chromatography ($CHCl_3$/CH_3OH, 99:1 to 90:10 as eluting solvent) to give a white-yellow powder (425 mg, 99.2% yield): R_f = 0.77 [$CHCl_3$/CH_3OH (90:10)]; ^{1}H NMR ($CDCl_3$) δ 4.02 (t, 4H), 4.71 (t, 4H), 7.32 (m, 2H), 8.38 (dd, 2H, J = 1.6 and 8.0 Hz), 8.60 (d, 2H, J = 4.4 Hz), 9.36 (s, 2H).

Tri(ethylene glycol) Di[3-(pyrid-3-yl)-1,2,5-thiadiazol-4-yl] Ether (8b). The crude compound was subsequently used without further purification (470 mg of pale-yellow powder, 99.5% yield): R_f = 0.72 [$CHCl_3$/CH_3OH (95:5)]; ^{1}H NMR ($CDCl_3$) δ 3.76 (s, 4H), 3.94 (t, 4H), 4.65 (t, 4H), 7.34 (m, 2H), 8.40 (d, 2H, J = 8.0 Hz), 8.60 (dd, 2H, J = 1.6 and 4.8 Hz), 9.38 (s, 2H).

Tetra(ethylene glycol) Di[3-(pyrid-3-yl)-1,2,5-thiadiazol-4-yl] Ether (8c). The crude oil was subsequently used without further purification (500 mg, 97% yield): R_f = 0.65 [EtOAc/hexane (50:50)]; ^{1}H NMR ($CDCl_3$) δ 3.69 (m, 8H), 3.92 (t, 4H), 4.66 (t, 4H), 7.38−7.40 (m, 2H), 8.43 (d, 2H, J = 8.1 Hz), 8.63 (dd, 2H, J = 1.6 and 4.8 Hz), 9.39 (s, 2H).

Penta(ethylene glycol) Di[3-(pyrid-3-yl)-1,2,5-thiadiazol-4-yl] Ether (8d). The crude compound was subsequently used without further purification (550 mg of yellow oil, 98.1% yield): R_f = 0.63 [$CHCl_3$/CH_3OH (95:5)]; ^{1}H NMR ($CDCl_3$) δ 3.62−3.71 (m, 12H), 3.93(m, 4H), 4.67 (m, 4H), 7.39 (m, 2H), 8.44 (d, 2H, J = 1.6 Hz), 8.64 (m, 2H), 9.39 (s, 2H).

Hexa(ethylene glycol) Di[3-(pyrid-3-yl)-1,2,5-thiadiazol-4-yl] Ether (8e). The crude yellow oil was purified by silica gel chromatography ($CHCl_3$/CH_3OH, 95:5 as eluting solvent) to give a yellow oil (600 mg, 99.2% yield): R_f = 0.67 [$CHCl_3$/CH_3OH (95:5)]; ^{1}H NMR ($CDCl_3$) δ 3.60−3.70 (m, 16H), 3.94 (t, 4H), 4.68 (t, 4H), 7.40 (m, 2H), 8.43 (d, 2H, J = 8.0 Hz), 8.64 (dd, 2H, J = 1.5 and 4.8 Hz), 9.40 (s, 2H).

Tri(propylene glycol) Di[3-(pyrid-3-yl)-1,2,5-thiadiazol-4-yl] Ether (8f). The crude compound was subsequently used without further purification (515 mg of dark-orange oil, 100% yield): R_f = 0.73 [$CHCl_3$/CH_3OH (95:5)]; ^{1}H NMR ($CDCl_3$) δ 1.10 (m, 6H), 1.43 (m, 4H), 3.50 (m, 2H), 3.70 (m, 4H), 5.25 (m, 2H), 7.37 (m, 2H), 8.40 (m, 2H), 8.62 (m, 2H), 9.38 (s, 2H).

General Procedure for the Preparation of Poly(ethylene glycol) Di[3-(1-methylpyridinium-3-yl)-1,2,5-thiadiazol-4-yl] Ether Diiodides (9). To a solution of poly(ethylene glycol) di[3-(pyrid-3-yl)-1,2,5-thiadiazol-4-yl] ether (1 mmol) in acetone (25 mL) was added CH_3I (3 mL, 48 mmol), and the solution was stirred under nitrogen for 36−48 h at room temperature. The resulting precipitate was filtered, washed with acetone, and dried under a vacuum; or if there was no precipitate, the solution was evaporated under reduced pressure to dryness to give the quaternary diiodide.

Di(ethylene glycol) Di[3-(1-methylpyridinium-3-yl)-1,2,5-thiadiazol-4-yl] ether diiodide (9a): pale-yellow powder (635 mg, 89.1% yield); ^{1}H NMR (DMSO-d_6) δ 4.02 (t, 4H), 4.46 (s, 6H), 4.69 (t, 4H), 8.25 (t, 2H), 9.05 (d, 4H, J = 7.2 Hz), 9.50 (s, 2H); ^{13}C NMR (DMSO-d_6) δ 48.5, 68.2, 70.8, 128.0, 130.0, 141.0, 141.8, 162.5.

Tri(ethylene glycol) di[3-(1-methylpyridinium-3-yl)-1,2,5-thiadiazol-4-yl] ether diiodide (9b): yellow powder (750 mg, 99.2% yield); mp 154−155 °C; ^{1}H NMR (DMSO-d_6) δ 3.66 (s, 4H), 3.88 (t, 4H), 4.45 (s, 6H, N−CH_3), 4.60 (t, 4H), 8.27 (t, 2H), 9.04 (d, 4H, J = 6.0 Hz), 9.49 (s, 2H); ^{13}C NMR ($CDCl_3$) δ 49.7, 68.4, 70.2, 70.4, 128.3, 130.9, 139.7, 142.2, 162.4.

Tetra(ethylene glycol) di[3-(1-methylpyridinium-3-yl)-1,2,5-thiadiazol-4-yl] ether diiodide (9c): pale-yellow powder (790 mg, 98.7% yield); mp 159−160.5 °C; ^{1}H NMR (DMSO-d_6) δ 3.53−3.61 (m, 8H), 3.88 (t, 4H), 4.46 (s, 6H, N−CH_3), 4.63 (t, 4H), 8.29 (t, 2H), 9.07 (d, 4H, J = 6.1 Hz), 9.51 (s, 2H); ^{13}C NMR (DMSO-d_6) δ 49.6, 68.1, 69.7, 70.8, 128.0, 130.1, 141.1, 141.8, 162.5. Anal. ($C_{24}H_{30}N_6O_5S_2I_2$) C, H, N.

Penta(ethylene glycol) di[3-(1-methylpyridinium-3-yl)-1,2,5-thiadiazol-4-yl] ether diiodide (9d): yellow oil (845 mg, 100% yield); ^{1}H NMR (DMSO-d_6) δ 3.46 (s, 4H), 3.52 (m, 4H), 3.61 (m, 4H), 3.88 (m, 4H), 4.47 (s, 6H),4.64 (t, 4H), 8.30 (t, 2H), 9.08 (d, 4H, J = 6.1 Hz), 9.51 (s, 2H); ^{13}C NMR (DMSO-d_6) δ 48.5, 68.1, 69.7, 70.7 127.9,130.1, 141.1, 141.8, 162.5.

Hexa(ethylene glycol) di[3-(1-methylpyridinium-3-yl)-1,2,5-thiadiazol-4-yl] ether diiodide (9e): yellow oil (890 mg, 100% yield); ^{1}H NMR (DMSO-d_6) δ 3.46 (m, 8H), 3.52 (m, 4H), 3.62 (m, 4H), 3.89 (t, 4H), 4.46 (s, 6H), 4.66 (t, 4H), 8.29 (m, 2H), 9.08 (m, 4H), 9.51 (s, 2H); ^{13}C NMR (DMSO-d_6) δ 48.5, 68.1, 69.6, 69.7, 70.8, 128.0, 130.1, 141.2, 141.8, 162.5.

Tri(propylene glycol) di[3-(1-methylpyridinium-3-yl)-1,2,5-thiadiazol-4-yl] ether diiodide (9f): yellow powder (800 mg, 100% yield); ^{1}H NMR (DMSO-d_6) δ 1.02 (m, 6H), 1.37 (m, 4H), 3.40 (m, 2H), 3.70 (m, 4H), 4.46 (s, 6H), 5.15 (m, 2H), 8.24 (m, 2H), 9.06 (s, 4H), 9.50 (s, 2H).

General Procedure for the Preparation of Poly(ethylene glycol) Di[3-(1-methyl-1,2,5,6-tetrahydropyrid-3-yl)-1,2,5-thiadiazol-4-yl] Ether Dihydrochlorides (11). The pyridinium iodide (approximately 1 mmol) was dissolved in a mixture of CH_3OH (15 mL) and $CHCl_3$ (15 mL). The solution was cooled to 0−5 °C, and $NaBH_4$ (154 mg, 4 mmol)

was added. After the mixture was stirred at 0−5 °C for 2 h, ice−water was added to the reaction mixture, which was then extracted with $CHCl_3$ twice. The combined organic extract was washed with water and dried over anhydrous Na_2SO_4. The solvent was removed under reduced pressure, and the residue was chromatographed on a column of silica gel using $CHCl_3$/CH_3OH (9:1) as eluent. The purified free base was redissolved in CH_3OH (10 mL) and was cooled to 0 °C. Then dry HCl gas was bubbled through the solution for 3 min, and the title compound was recrystallized from CH_3OH/ether.

Di(ethylene glycol) di[3-(1-methyl-1,2,5,6-tetrahydropyrid-3-yl)-1,2,5-thiadiazol-4-yl] ether dihydrochloride (CDD-0274-A) (11a): Reduction of the quaternary salt (600 mg, 0.84 mmol) yielded the dihydrochloride (212 mg, as pale-white powder, 47.0% yield); mp 193−194 °C; ^{1}H NMR (D_2O) δ 2.41 (m, 4H), 2.81 (s, 6H, N−CH_3), 3.02 (m, 2H), 3.37 (m, 2H), 3.75 (m, 2H), 3.84 (t, 4H), 4.19 (m, 2H), 4.44 (m, 4H), 6.93 (s, 2H, vinylic); ^{13}C NMR (D_2O/CD_3OD) δ 23.5, 43.5, 50.9, 52.8, 70.0, 71.3, 124.2, 129.1, 145.7, 163.2. Anal. ($C_{20}H_{28}N_6O_3S_2$·2HCl·H_2O) C, H, N.

Tri(ethylene glycol) di[3-(1-methyl-1,2,5,6-tetrahydropyrid-3-yl)-1,2,5-thiadiazol-4-yl] ether dihydrochloride (CDD-0272-A) (11b): Reduction of the quaternary salt (750 mg, 0.99 mmol) yielded the dihydrochloride (170 mg, as yellow-white powder, 29.2% yield); mp 111−112 °C; ^{1}H NMR (D_2O) δ 2.49 (m, 4H), 2.82 (s, 6H, N−CH_3), 3.04 (m, 2H), 3.40 (m, 2H), 3.56 (s, 4H), 3.74 (m, 6H), 4.22 (m, 2H), 4.38 (s, 4H), 7.00 (s, 2H, vinylic); ^{13}C NMR (D_2O/CD_3OD) δ 23.5, 43.5, 50.9, 52.9, 69.8, 70.9, 71.1, 124.2, 129.2, 145.8, 163.1. Anal. ($C_{22}H_{32}N_6O_4S_2$·2HCl·H_2O) C, H, N.

Tetra(ethylene glycol) di[3-(1-methyl-1,2,5,6-tetrahydropyrid-3-yl)-1,2,5-thiadiazol-4-yl] ether dihydrochloride (CDD-0273-A) (11c): Reduction of the quaternary salt (750 mg, 0.94 mmol) yielded the dihydrochloride (300 mg, as yellow-white powder, 51% yield); mp 69.2−70.8 °C; free base R_f = 0.60 [$CHCl_3$/CH_3OH (9:1)]; ^{1}H NMR (D_2O) δ 2.48 (m, 4H), 2.81 (s, 6H, N−CH_3), 3.04 (m, 2H), 3.50 (m, 10H), 3.75 (m, 6H), 4.23 (m, 2H), 4.37 (s, 4H), 7.00 (s, 2H, vinylic); ^{13}C NMR ($CDCl_3$) δ 23.0, 43.4, 50.0, 51.9, 69.3, 70.3, 70.8, 123.8, 127.5, 144.3, 162.3. Anal. ($C_{24}H_{36}N_6O_5S_2$·2HCl·H_2O) C, H, N.

Penta(ethylene glycol) di[3-(1-methyl-1,2,5,6-tetrahydropyrid-3-yl)-1,2,5-thiadiazol-4-yl] ether dihydrochloride (CDD-0279-A) (11d): Reduction of the quaternary salt (840 mg, 1.0 mmol) yielded the dihydrochloride (300 mg, as white-yellow powder, 44.8% yield); mp 88−89 °C (hygroscopic); ^{1}H NMR (D_2O) δ 2.52 (m, 4H), 2.83 (s, 6H, N−CH_3), 3.06 (m, 2H), 3.41−3.50 (m, 12H), 3.55 (m, 4H), 3.75 (t, 4H), 3.85 (d, 2H), 4.37 (d, 2H), 4.43 (t, 4H), 7.04 (s, 2H, vinylic); ^{13}C NMR (D_2O/CD_3OD) δ 23.5, 43.5, 50.9, 52.9, 69.9, 70.7, 70.9, 71.0, 124.2, 129.2, 145.9, 163.2. Anal. ($C_{26}H_{40}N_6O_6S_2$·2HCl·0.5H_2O) C, H, N.

Hexa(ethylene glycol) di[3-(1-methyl-1,2,5,6-tetrahydropyrid-3-yl)-1,2,5-thiadiazol-4-yl] ether dihydrochloride (CDD-0283-A) (11e): Reduction of the quaternary salt (880 mg, 0.99 mmol) yielded the dihydrochloride (280 mg, as brown powder, 39.6% yield); mp 60−62 °C (hygroscopic); ^{1}H NMR (D_2O) δ 2.52 (m, 4H), 2.83 (s, 6H, N−CH_3), 3.06 (m, 2H), 3.42−3.48 (m, 16H), 3.52 (m, 4H), 3.75 (t, 4H), 3.80 (d, 2H), 4.25 (d, 2H), 4.42 (t, 4H), 7.03 (s, 2H, vinylic); ^{13}C NMR (D_2O/CD_3OD) δ 23.6, 43.5, 50.9, 52.9, 69.9, 70.7, 70.9, 71.1, 124.2, 129.2, 145.9, 163.2. Anal. ($C_{28}H_{44}N_6O_7S_2$·2HCl·$2H_2O$) C, H, N.

Tri(propylene glycol) di[3-(1-methyl-1,2,5,6-tetrahydropyrid-3-yl)-1,2,5-thiadiazol-4-yl] ether dihydrochloride (CDD-0281-A) (11f): Reduction of the quaternary salt (790 mg, 0.99 mmol) yielded the dihydrochloride (286 mg, as yellow powder, 46.4% yield); mp 32−34 °C (hygroscopic); ^{1}H NMR (D_2O) δ 0.95−1.14 (m, 10H), 2.75 (m, 4H), 2.85 (s, 6H, N−CH_3), 3.10 (m, 2H), 3.40−3.60 (m, 8H), 3.80 (m, 2H), 4.23 (m, 2H), 4.98 (m, 2H), 7.05 (s, 2H, vinylic); ^{13}C NMR (D_2O/CD_3OD) δ 16.7, 23.5, 43.5, 50.9, 52.9, 72.6, 74.8, 124.3, 129.2, 146.1, 162.6. Anal. ($C_{25}H_{38}N_6O_4S_2$·2HCl·$2H_2O$) C, H, N.

General Procedure for the Preparation of Bis[3-(pyrid-3-yl)-1,2,5-thiadiazol-4-ylthio]alkanes (13). 3-(3-Chloro-1,2,5-thiadiazol-4-yl)pyridine (500 mg, 2.53 mmol) was dissolved in a mixture of THF and DMF. Sodium hydrogen sulfide monohydrate (280 mg, 3.80 mmol) was added. After the mixture was stirred at room temperature for 2 h, potassium carbonate (700 mg, 5.06 mmol) was added and the reaction mixture was stirred at room temperature for another 1 h. Then the appropriate dibromo compound (1.0 mmol) was added and the reaction mixture was stirred at room temperature overnight. Then ice was added and the solution was extracted with $CHCl_3$. The $CHCl_3$ extract was dried over Na_2SO_4 and evaporated in vacuo. The residue was chromatographed on a column of silica gel (eluting with appropriate solvents) to give compound **1**.

1,2-Bis[3-(pyrid-3-yl)-1,2,5-thiadiazol-4-ylthio]ethane (13a): pale-white crystal (226 mg, 54.3% yield, hexane/EtOAc 1:1 as eluent); mp 153−154 °C; R_f = 0.50 [hexane/EtOAc (1:1)]; ^{1}H NMR ($CDCl_3$) δ 3.77 (t, 4H), 7.44 (m, 2H), 8.20 (d, 2H, J = 8.0), 8.71 (d, 2H, J = 4.8 Hz), 9.16 (s, 2H).

1,3-Bis[3-(pyrid-3-yl)-1,2,5-thiadiazol-4-ylthio]propane (13b): white powder (375 mg, 87.1% yield, recrystallized from hexane/EtOAc); mp 86.4−88 °C; R_f = 0.46 [hexane/EtOAc (1:1)]; ^{1}H NMR ($CDCl_3$) δ 2.34 (m, 2H), 3.48 (t, 4H), 7.43 (m, 2H), 8.22 (d, 2H, J = 8.0 Hz), 8.71 (d, 2H, J = 4.6 Hz), 9.18 (s, 2H).

1,4-Bis[3-(pyrid-3-yl)-1,2,5-thiadiazol-4-ylthio]butane (13c): white powder (260 mg, 58.5% yield, recrystallized from hexane/EtOAc); mp 96.4−98.0 °C; R_f = 0.40 [hexane/EtOAc (1:1)]; ^{1}H NMR ($CDCl_3$) δ 2.00 (m, 4H), 3.39 (t, 4H), 7.43 (m, 2H), 8.21 (dd, 2H, J = 1.6 and 8.0 Hz), 8.70 (d, 2H, J = 4.8 Hz), 9.17 (s, 2H); ^{13}C NMR ($CDCl_3$) δ 28.1, 32.5, 123.3, 128.1, 135.5, 149.3, 150.5, 155.2, 156.3.

1,5-Bis[3-(pyrid-3-yl)-1,2,5-thiadiazol-4-ylthio]pentane (13d): yellow crystal (300 mg, 65.4% yield, recrystallized from hexane/EtOAc); mp 74−75 °C; R_f = 0.46 [hexane/EtOAc (1:1)]; ^{1}H NMR ($CDCl_3$) δ 1.65 (m, 2H), 1.87 (m, 4H), 3.34 (t, 4H), 7.43 (m, 2H), 8.22 (dd, 2H, J = 1.6 and 8.0 Hz), 8.70 (d, 2H, J = 4.8 Hz), 9.18 (s, 2H).

1,6-Bis[3-(pyrid-3-yl)-1,2,5-thiadiazol-4-ylthio]hexane (13e): yellow powder (360 mg, 76.2% yield, recrystallized from hexane/EtOAc); mp 62−62.5 °C; R_f = 0.50 [hexane/EtOAc (1:1)]; ^{1}H NMR ($CDCl_3$) δ 1.53 (m, 4H), 1.83 (m, 4H), 3.33 (t, 4H), 7.43 (m, 2H), 8.23 (dd, 2H, J = 1.6 and 8.0 Hz), 8.70 (d, 2H, J = 4.8 Hz), 9.18 (s, 2H).

1,7-Bis[3-(pyrid-3-yl)-1,2,5-thiadiazol-4-ylthio]heptane (13f): White-yellow powder (303 mg, 62.3% yield, recrystallized from hexane/EtOAc); mp 45.3−47.0 °C; R_f = 0.42 [hexane/EtOAc (1:1)]; ^{1}H NMR ($CDCl_3$) δ 1.45 (m, 6H), 1.80 (m, 4H), 3.32 (t, 4H), 7.44 (m, 2H), 8.23 (d, 2H, J = 8.0 Hz), 8.70 (dd, 2H, J = 1.6 and 4.8 Hz), 9.18 (s, 2H).

1,8-Bis[3-(pyrid-3-yl)-1,2,5-thiadiazol-4-ylthio]octane (13g): White-yellow powder (323 mg, 64.5% yield, recrystallized from hexane/EtOAc); mp 46.5−48.4 °C; R_f = 0.39 [hexane/EtOAc (1:1)]; ^{1}H NMR ($CDCl_3$) δ 1.36−1.47 (m, 8H), 1.80 (m, 4H), 3.32 (t, 4H), 7.43 (m, 2H), 8.23 (dd, 2H, J = 1.6 and 8.0 Hz), 8.70 (d, 2H, J = 4.8 Hz), 9.18 (s, 2H).

1,9-Bis[3-(pyrid-3-yl)-1,2,5-thiadiazol-4-ylthio]nonane (13h): yellow-white powder (290 mg, 56.3% yield, recrystallized from hexane/EtOAc); mp 33−34 °C; R_f = 0.57 [hexane/EtOAc (1:1)]; ^{1}H NMR ($CDCl_3$) δ 1.36−1.47 (m, 10H), 1.80 (m, 4H), 3.32 (t, 4H), 7.43 (m, 2H), 8.23 (dd, 2H, J = 1.6 and 8.0 Hz), 8.70 (d, 2H, J = 4.8 Hz), 9.18 (s, 2H); ^{13}C NMR ($CDCl_3$) δ 28.8, 28.9, 29.0, 29.2, 33.1, 123.3, 128.2, 135.5, 149.4, 150.5, 155.2, 156.8.

1,10-Bis[3-(pyrid-3-yl)-1,2,5-thiadiazol-4-ylthio]decane (13i): colorless oil (450 mg, 85.1% yield, hexane/EtOAc 1:1 as eluent); R_f = 0.56 [hexane/EtOAc (1:1)]; ^{1}H NMR ($CDCl_3$) δ 1.25−1.55 (m, 12H), 1.78 (m, 4H), 3.32 (t, 4H), 7.42 (m, 2H), 8.23 (d, 2H, J = 8.0 Hz), 8.69 (d, 2H, J = 4.8 Hz), 9.18 (s, 2H).

1,11-Bis[3-(pyrid-3-yl)-1,2,5-thiadiazol-4-ylthio]undecane (13j): colorless oil (435 mg, 80.1% yield, hexane/EtOAc 1:1 as eluent); R_f = 0.57 [hexane/EtOAc (1:1)]; ^{1}H NMR ($CDCl_3$) δ 1.28−1.45 (m, 14H), 1.78 (m, 4H), 3.31 (t, 4H), 7.40 (m, 2H), 8.22 (d, 2H, J = 8.0 Hz), 8.69 (d, 2H, J = 4.8 Hz), 9.18 (s, 2H).

1,12-Bis[3-(pyrid-3-yl)-1,2,5-thiadiazol-4-ylthio]dodecane (13k): white crystal (400 mg, 71.8% yield) (hexane/

EtOAc 3:1 as eluent); mp 37−38 °C; $R_f = 0.78$ [hexane/EtOAc (1:1)]; ^{1}H NMR ($CDCl_3$) δ 1.27−1.46 (m, 16H), 1.79 (m, 4H), 3.32 (t, 4H), 7.43 (m, 2H), 8.24 (dd, 2H, J = 1.6 and 8.0 Hz), 8.70 (d, 2H, J = 4.8 Hz), 9.19 (s, 2H). Anal. ($C_{26}H_{32}N_6S_4$) C, H, N.

General Procedure for the Preparation of Quaternary Salts of Bis[3-(pyrid-3-yl)-1,2,5-thiadiazol-4-ylthio]alkanes (14). To a solution of an appropriate compound **13** in a mixture of acetone and $CHCl_3$ was added excess CH_3I (4 equiv), and the solution was stirred for 36 h at room temperature. The reaction mixture was concentrated in vacuo to give the crude product **14**, which was sufficiently pure for the next reaction step.

1,2-Bis[3-(1-methylpyridinium-3-yl)-1,2,5-thiadiazol-4-ylthio]ethane diiodide (14a): Addition of CH_3I to **13a** (220 mg) yielded **14a** (350 mg, yellow powder, 94.6% yield); ^{1}H NMR (DMSO-d_6) δ 3.77 (t, 4H), 4.45 (s, 6H, N−CH_3), 8.34 (m, 2H), 8.95 (d, 2H, J = 8.2 Hz), 9.12 (d, 2H, J = 5.6 Hz), 9.44 (s, 2H); ^{13}C NMR (DMSO-d_6) δ 32.2, 48.4, 127.8, 130.7, 143.1, 151.7, 155.8.

1,3-Bis[3-(1-methylpyridinium-3-yl)-1,2,5-thiadiazol-4-ylthio]propane diiodide (14b): Addition of CH_3I to **13b** (375 mg) yielded **14b** (620 mg, yellow powder, 99.6% yield); ^{1}H NMR (DMSO-d_6) δ 2.25 (m, 1H), 2.85 (m, 1H), 3.50 (t, 4H), 4.45 (s, 6H, N−CH_3), 8.32 (m, 2H), 8.95 (d, 2H, J = 8.0 Hz), 9.15 (d, 2H, J = 6.0 Hz), 9.45 (s, 2H); ^{13}C NMR (DMSO-d_6) δ 27.8, 31.5, 48.5, 127.8, 130.7, 143.1, 151.6, 156.5.

1,4-Bis[3-(1-methylpyridinium-3-yl)-1,2,5-thiadiazol-4-ylthio]butane diiodide (14c): Addition of CH_3I to **13c** (260 mg) yielded **14c** (415 mg, yellow powder, 97.4% yield); mp 172−174 °C; ^{1}H NMR (DMSO-d_6) δ 1.91 (m, 4H), 3.41 (t, 4H), 4.46 (s, 6H, N−CH_3), 8.33 (m, 2H), 8.97 (d, 2H, J = 7.2 Hz), 9.12 (d, 2H, J = 5.3 Hz), 9.45 (s, 2H); ^{13}C NMR (DMSO-d_6) δ 27.6, 32.2, 48.5, 127.8, 130.8, 143.1, 151.5, 156.7.

1,5-Bis[3-(1-methylpyridinium-3-yl)-1,2,5-thiadiazol-4-ylthio]pentane diiodide (14d): Addition of CH_3I to **13d** (300 mg) yielded **14d** (485 mg, brown oil, 99.9% yield); ^{1}H NMR (DMSO-d_6) δ 1.37 (m, 2H), 1.79 (m, 4H), 3.39 (t, 4H), 4.46 (s, 6H, N−CH_3), 8.33 (m, 2H), 8.98 (d, 2H, J = 8.0 Hz), 9.12 (d, 2H, J = 6.0 Hz), 9.45 (s, 2H); ^{13}C NMR (DMSO-d_6) δ 27.3. 28.0, 32.6, 48.5, 127.8, 130.8, 143.1, 151.5, 156.9.

1,6-Bis[3-(1-methylpyridinium-3-yl)-1,2,5-thiadiazol-4-ylthio]hexane diiodide (14e): Addition of CH_3I to **13e** (360 mg) yielded **14e** (575 mg, yellow powder, 99.8% yield); mp 187.3−188.9 °C; ^{1}H NMR (DMSO-d_6) δ 1.46 (m, 4H), 1.76 (m, 4H), 3.38 (t, 4H), 4.45 (s, 6H, N−CH_3), 8.32 (m, 2H), 8.97 (d, 2H, J = 8.2 Hz), 9.12 (d, 2H, J = 6.0 Hz), 9.44 (s, 2H); ^{13}C NMR (DMSO-d_6) δ 27.6, 28.4, 32.7, 48.5, 127.8, 130.8, 143.1, 151.5, 157.0.

1,7-Bis[3-(1-methylpyridinium-3-yl)-1,2,5-thiadiazol-4-ylthio]heptane diiodide (14f): Addition of CH_3I to **13f** (303 mg) yielded **14f** (475 mg, yellow powder, 99.0% yield); mp 109.2−110.8 °C; ^{1}H NMR (DMSO-d_6) δ 1.39 (m, 6H), 1.75 (m, 4H), 3.37 (t, 4H), 4.46 (s, 6H, N−CH_3), 8.33 (m, 2H), 8.98 (d, 2H, J = 8.2 Hz), 9.12 (d, 2H, J = 6.0 Hz), 9.45 (s, 2H); ^{13}C NMR (DMSO-d_6) δ 28.0, 28.4, 32.7, 48.5, 127.8, 130.8, 143.0, 151.5, 157.0.

1,8-Bis[3-(1-methylpyridinium-3-yl)-1,2,5-thiadiazol-4-ylthio]octane diiodide (14g): Addition of CH_3I to **13g** (320 mg) yielded **14g** (500 mg, puffy yellow powder, 99.7% yield); ^{1}H NMR (DMSO-d_6) δ 1.30−1.42 (m, 8H), 1.74 (m, 4H), 3.37 (t, 4H), 4.45 (s, 6H, N−CH_3), 8.33 (m, 2H), 8.98 (d, 2H, J = 8.2 Hz), 9.12 (d, 2H, J = 6.0 Hz), 9.44 (s, 2H); ^{13}C NMR (DMSO-d_6) δ 28.1, 28.3, 28.5, 32.8, 48.5, 127.8, 130.8, 143.0, 151.5, 157.0.

1,9-Bis[3-(1-methylpyridinium-3-yl)-1,2,5-thiadiazol-4-ylthio]nonane diiodide (14h): Addition of CH_3I to **13h** (290 mg) yielded **14h** (450 mg, yellow oil, 99.9% yield); ^{1}H NMR (DMSO-d_6) δ 1.27−1.40 (m, 10H), 1.74 (m, 4H), 3.34 (t, 4H), 4.45 (s, 6H, N−CH_3), 8.30 (m, 2H), 8.97 (d, 2H, J = 7.9 Hz), 9.11 (d, 2H, J = 5.7 Hz), 9.44 (s, 2H); ^{13}C NMR (DMSO-d_6) δ 28.1, 28.5, 32.8, 48.4, 127,8, 130.8, 143.1, 151.5, 157.0.

1,10-Bis[3-(1-methylpyridinium-3-yl)-1,2,5-thiadiazol-4-ylthio]decane diiodide (14i): Addition of CH_3I to **13i** (450 mg) yielded **14i** (600 mg, yellow oil, 86.8% yield); ^{1}H NMR (DMSO-d_6) δ 1.26−1.40 (m, 10H), 1.74 (m, 4H), 3.33 (t, 4H), 4.44 (s, 6H, N−CH_3), 8.32 (m, 2H), 8.87 (d, 2H, J = 8.0 Hz), 9.11 (d, 2H, J = 6.4 Hz), 9.44 (s, 2H); ^{13}C NMR (DMSO-d_6) δ 28.2, 28.5, 28.8, 32.8, 48.4, 127.8, 130.8, 143.1, 143.6, 151.5, 157.0.

1,11-Bis[3-(1-methylpyridinium-3-yl)-1,2,5-thiadiazol-4-ylthio]undecane diiodide (14j): Addition of CH_3I to **13j** (435 mg) yielded **14j** (600 mg, orange oil, 90.6% yield); ^{1}H NMR (DMSO-d_6) δ 1.25−1.40 (m, 14H), 1.74 (m, 4H), 3.32 (t, 4H), 4.45 (s, 6H, N−CH_3), 8.33 (m, 2H), 8.98 (d, 2H, J = 8.1 Hz), 9.12 (d, 2H, J = 6.0 Hz), 9.45 (s, 2H).

1,12-Bis[3-(1-methylpyridinium-3-yl)-1,2,5-thiadiazol-4-ylthio]dodecane diiodide (14k): Addition of CH_3I to **13k** (400 mg) yielded **14k** (600 mg, yellow powder, 99.4% yield); ^{1}H NMR (DMSO-d_6) δ 1.40−1.50 (m, 16H), 1.73 (m, 4H), 3.35 (t, 4H), 4.45 (s, 6H, N−CH_3), 8.32 (m, 2H), 8.96 (d, 2H, J = 8.0 Hz), 9.11 (d, 2H, J = 6.1 Hz), 9.44 (s, 2H); ^{13}C NMR (DMSO-d_6) δ 28.2, 28.5, 29.0, 32.8, 48.5, 127.8, 130.8, 143.1, 151.5, 157.0.

General Procedure for the Preparation of Bis[3-(1-methyl-1,2,5,6-tetrahydropyrid-3-yl)-1,2,5-thiadiazol-4-ylthio]alkane Dihydrochlorides (16). Compound **12** was dissolved in a mixture of $CHCl_3$ and CH_3OH (1:1). The solution was cooled to 0−5 °C, and $NaBH_4$ (4.0 equivalent) was added. The mixture was stirred at 0−5 °C for 2 h, then ice was added and the mixture was extracted with $CHCl_3$. The $CHCl_3$ extract was dried over Na_2SO_4 and evaporated in vacuo. The residue was chromatographed on a column of silica gel (5−10% CH_3OH in $CHCl_3$ as eluent). The purified compound was dissolved in $CH_3OH/CHCl_3$ and cooled to 0 °C. Then dry HCl was bubbled through the solution for 5 min and cold ether was added to precipitate the dihydrochloride. The precipitated solid was filtered, washed with ether, and dried to give the title compound **16**.

1,2-Bis[3-(1-methyl-1,2,5,6-tetrahydropyrid-3-yl)-1,2,5-thiadiazol-4-ylthio]ethane dihydrochloride (CDD-0280-A) (16a): Reduction of the quaternary salt **14a** (350 mg, 0.50 mmol) yielded the dihydrochloride **16a** (88 mg, as a pale yellow-white powder, 33.5% yield); mp 206−207 °C; ^{1}H NMR (D_2O) δ 2.53 (m, 4H), 2.83 (s, 6H, N−CH_3), 3.12 (m, 2H), 3.42 (m, 2H), 3.51 (m, 4H), 3.80 (m, 2H), 4.22 (m, 2H), 6.68 (s, 2H, vinylic); ^{13}C NMR (D_2O/CD_3OD) δ 23.5, 33.2, 43.4, 50.8, 53.4, 124.6, 130.4, 155.7, 156.4. Anal. ($C_{18}H_{24}N_6S_4 \cdot 2HCl \cdot H_2O$) C, H, N.

1,3-Bis[3-(1-methyl-1,2,5,6-tetrahydropyrid-3-yl)-1,2,5-thiadiazol-4-ylthio]propane dihydrochloride (CDD-0284-A) (16b): Reduction of the quaternary salt **14b** (615 mg, 0.86 mmol) yielded the dihydrochloride **16b** (203 mg, as a pale white-yellow powder, 43.7% yield); mp 133−135 °C; ^{1}H NMR (D_2O) δ 2.00 (m, 2H), 2.56 (m, 4H), 2.84 (s, 6H, N−CH_3), 3.12 (m, 2H), 3.23 (m, 4H), 3.44 (m, 2H), 3.81 (m, 2H), 4.24 (m, 2H), 6.75 (s, 2H, vinylic); ^{13}C NMR (D_2O/CD_3OD) δ 23.6, 28.7, 32.4, 43.5, 50.9, 53.5, 124.7, 130.6, 155.9, 157.1. Anal. ($C_{19}H_{26}N_6S_4 \cdot 2HCl \cdot H_2O$) C, H, N.

1,4-Bis[3-(1-methyl-1,2,5,6-tetrahydropyrid-3-yl)-1,2,5-thiadiazol-4-ylthio]butane dihydrochloride (CDD-0285-A) (16c): Reduction of the quaternary salt **14c** (415 mg, 0.57 mmol) yielded the dihydrochloride **16c** (120 mg, as a pale white-yellow powder, 38.0% yield); mp 215−216.6 °C; ^{1}H NMR (D_2O) δ 1.71 (m, 4H), 2.55 (m, 4H), 2.84 (s, 6H, N−CH_3), 3.12 (m, 6H), 3.43 (m, 2H), 3.79 (m, 2H), 4.24 (m, 2H), 6.71 (s, 2H, vinylic); ^{13}C NMR (D_2O/CD_3OD) δ 23.6, 28.2, 33.2, 43.5, 50.9, 53.5, 124.7, 130.5, 155.8, 157.4. Anal. ($C_{20}H_{28}N_6S_4 \cdot 2HCl \cdot 0.5Et_2O$) C, H, N.

1,5-Bis[3-(1-methyl-1,2,5,6-tetrahydropyrid-3-yl)-1,2,5-thiadiazol-4-ylthio]pentane dihydrochloride (CDD-0286-A) (16d): Reduction of the quaternary salt **14d** (480 mg, 0.65 mmol) yielded the dihydrochloride **16d** (179 mg, as a white-yellow powder, 48.8% yield); mp 187.2−189.4 °C; ^{1}H NMR (D_2O) δ 1.39 (m, 2H), 1.59 (m, 4H), 2.56 (m, 4H), 2.85 (s, 6H, N−CH_3), 3.10 (m, 6H), 3.44 (m, 2H), 3.81 (m, 2H), 4.24 (m, 2H), 6.75 (s, 2H, vinylic); ^{13}C NMR (D_2O/CD_3OD) δ 23.5, 28.0, 28.8, 33.5, 43.4, 50.8, 53.4, 124.7, 130.3, 155.6, 157.6. Anal. ($C_{21}H_{30}N_6S_4 \cdot 2HCl$) C, H, N.

1,6-Bis[3-(1-methyl-1,2,5,6-tetrahydropyrid-3-yl)-1,2,5-thiadiazol-4-ylthio]hexane dihydrochloride (CDD-0287-A) (16e): Reduction of the quaternary salt **14e** (570 mg, 0.75 mmol) yielded the dihydrochloride **16e** (126 mg, as a yellow powder, 28.7% yield); mp 233.1−235.5 °C; ^{1}H NMR (D_2O) δ 1.24 (m, 4H), 1.52 (m, 4H), 2.56 (m, 4H), 2.85 (s, 6H, N−CH_3), 3.06 (m, 6H), 3.44 (m, 2H), 3.80 (m, 2H), 4.24 (m, 2H), 6.75 (s, 2H, vinylic); ^{13}C NMR (D_2O/CD_3OD) δ 23.4, 28.2, 29.0, 33.5, 43.3, 50.6, 53.2, 124.5, 130.2, 155.3, 157.4. Anal. ($C_{22}H_{32}N_6S_4$·2HCl) C, H, N.

1,7-Bis[3-(1-methyl-1,2,5,6-tetrahydropyrid-3-yl)-1,2,5-thiadiazol-4-ylthio]heptane dihydrochloride (CDD-0288-A) (16f): Reduction of the quaternary salt **14f** (470 mg, 0.61 mmol) yielded the dihydrochloride **16f** (198 mg, as a white powder, 54.5% yield); mp 200.5−202.8 °C; ^{1}H NMR (D_2O) δ 1.21 (m, 6H), 1.54 (m, 4H), 2.57 (m, 4H), 2.84 (s, 6H, N−CH_3), 3.10 (t, 6H), 3.43 (m, 2H), 3.82 (m, 2H), 4.24 (m, 2H), 6.76 (s, 2H, vinylic); ^{13}C NMR (D_2O/CD_3OD) δ 23.5, 28.7, 29.2, 33.8, 43.4, 50.8, 53.4, 124.7, 130.3, 155.6, 157.7. Anal. ($C_{23}H_{34}N_6S_4$·2HCl) C, H, N.

1,8-Bis[3-(1-methyl-1,2,5,6-tetrahydropyrid-3-yl)-1,2,5-thiadiazol-4-ylthio]octane dihydrochloride (CDD-0289-A) (16g): Reduction of the quaternary salt **14g** (500 mg, 0.64 mmol) yielded the dihydrochloride **16g** (176 mg, as a pale white-yellow powder, 45.3% yield); mp 190.1−192.5 °C; ^{1}H NMR (D_2O) δ 1.11−1.24 (m, 8H), 1.54 (m, 4H), 2.58 (m, 4H), 2.85 (s, 6H, N−CH_3), 3.10 (t, 6H), 3.45 (m, 2H), 3.82 (m, 2H), 4.25 (m, 2H), 6.77 (s, 2H, vinylic); ^{13}C NMR (D_2O/CD_3OD) δ 23.5, 28.7, 28.9, 29.2, 33.8, 43.4, 50.8, 53.4, 124.7, 130.3, 155.6, 157.7. Anal. ($C_{24}H_{36}N_6S_4$·2HCl) C, H, N.

1,9-Bis[3-(1-methyl-1,2,5,6-tetrahydropyrid-3-yl)-1,2,5-thiadiazol-4-ylthio]nonane dihydrochloride (CDD-0290-A) (16h): Reduction of the quaternary salt **14h** (445 mg, 0.56 mmol) yielded the dihydrochloride **16h** (220 mg, as a yellow powder, 63.3% yield); mp 119.8−121.5 °C; ^{1}H NMR (D_2O) δ 1.06−1.18 (m, 10H), 1.49 (m, 4H), 2.53 (m, 4H), 2.82 (s, 6H, N−CH_3), 2.98 (m, 6H), 3.42 (m, 2H), 3.78 (m, 2H), 4.18 (m, 2H), 6.66 (s, 2H, vinylic); ^{13}C NMR (D_2O/CD_3OD) δ 23.5, 29.6, 33.9, 43.4, 50.5, 53.1, 124.8, 130.2, 155.1, 157.3. Anal. ($C_{25}H_{38}N_6S_4$·2HCl) C, H, N.

1,10-Bis[3-(1-methyl-1,2,5,6-tetrahydropyrid-3-yl)-1,2,5-thiadiazol-4-ylthio]decane dihydrochloride (CDD-0277-A) (16i): Reduction of the quaternary salt **14i** (600 mg, 0.74 mmol) yielded the dihydrochloride **16i** (200 mg, as a pale yellow-white powder, 42.2% yield); mp 144−145 °C; ^{1}H NMR (D_2O) δ 1.05−1.20 (m, 12H), 1.47 (m, 4H), 2.51 (m, 4H), 2.79 (s, 6H, N−CH_3), 3.03 (m, 4H), 3.40 (m, 2H), 3.75 (m, 2H), 4.20 (m, 2H), 6.71 (s, 2H, vinylic); ^{13}C NMR (D_2O/CD_3OD) δ 23.6, 29.2,29.4, 29.7, 33.9, 43.5, 50.8, 53.4, 124.8, 130.3, 155.4, 157.6. Anal. ($C_{26}H_{40}N_6S_4$·2HCl·0.5H_2O) C, H, N.

1,11-Bis[3-(1-methyl-1,2,5,6-tetrahydropyrid-3-yl)-1,2,5-thiadiazol-4-ylthio]undecane dihydrochloride (CDD-0278-A) (16j): Reduction of the quaternary salt **14j** (600 mg, 0.72 mmol) yielded the dihydrochloride **16j** (181 mg, as a pale white-yellow powder, 38.2% yield); mp 100−102 °C; ^{1}H NMR (D_2O) δ 1.01−1.16 (m, 14H), 1.47 (m, 4H), 2.52 (m, 4H), 2.80 (s, 6H, N−CH_3), 3.01 (t, 4H), 3.20 (m, 4H), 4.00 (m, 4H), 6.70 (s, 2H, vinylic); ^{13}C NMR (D_2O/CD_3OD) δ 23.6, 29.6,29.7, 30.1, 34.0, 43.5, 50.7, 53.3, 125.0, 130.3, 155.3, 157.5. Anal. ($C_{27}H_{42}N_6S_4$·2HCl·0.5H_2O) C, H, N.

1,12-Bis[3-(1-methyl-1,2,5,6-tetrahydropyrid-3-yl)-1,2,5-thiadiazol-4-ylthio]dodecane dihydrochloride (CDD-0276-A) (16k): Reduction of the quaternary salt **14k** (600 mg, 0.71 mmol) yielded the dihydrochloride **16k** (236 mg, as a pale-yellow powder, 49.7% yield); mp 155−157 °C; ^{1}H NMR (D_2O) δ 1.07−1.25 (m, 16H), 1.50 (m, 4H), 2.55 (m, 4H), 2.81 (s, 6H, N−CH_3), 2.95 (m, 4H), 3.20 (m, 4H), 3.98 (m, 4H), 6.82 (s, 2H, vinylic); ^{13}C NMR (D_2O/CD_3OD) δ 23.7, 30.0, 30.2, 30.6, 34.0, 43.5, 50.6, 53.2, 125.1, 130.2, 155.1, 157.3. Anal. ($C_{28}H_{44}N_6S_4$·2HCl·0.5H_2O) C, H, N.

Receptor Assays. The M_1, M_3, and M_5 subtypes of muscarinic receptor couple efficiently to phospholipase Cβ via the $G_{q/11}$ family of G proteins. Compounds were examined for their abilities to activate G proteins by measuring accumulation of [^{3}H]-inositol phosphates in stably transfected cells (A9 L cells and/or NIH 3T3 cells) upon agonist stimulation as described previously.[18,22,23,26,27] Cells were transfected with plasmids containing the genes for human M_1 or M_5 receptors (provided by Dr. Tom Bonner of the National Institutes of Health).[28,29] Activity is presented as the percentage activation above basal levels. Carbachol was utilized in each assay as a positive control for muscarinic receptor activation.

Membrane homogenates were prepared from transfected cells using established procedures.[18,22,23,30] All binding assays were conducted in a 1 mL mixture of binding buffer [25 mM sodium phosphate (pH 7.4) containing 5 mM magnesium chloride]. In saturation binding assays, eight concentrations of [^{3}H]-(*R*)-quinuclidinyl benzilate (QNB) were used ranging from 5 to 300 pM. In ligand inhibition binding assays, 0.1 nM of [^{3}H]-(*R*)-QNB and 14 points for the test ligand (ranging from 0.01 nM to 3 mM) were used. The mixture was incubated for 2 h at room temperature. Total binding and nonspecific binding were determined in the absence and presence of a 1000-fold excess of unlabeled (*R*)-QNB. Radioactivity was counted using either a 6895 BetaTrac liquid scintillation counter (TM Analytic, Elk Grove Village, IL) or a TopCount NXT system (Packard, Meriden, CT). Consistent results were obtained from both systems for saturation binding and inhibition binding assays.

M_4 agonist activity was measured on a subclone of the RBL-2H3 mast cell line that was stably transfected with the human M_4 receptor at $>1 \times 10^5$ r/c. Compounds were tested for their ability to trigger degranulation and release of hexosaminidase into the supernatant, similar to procedures previously described for the M_1 receptor.[31]

Data Analysis. Nonlinear least squares curve-fitting was performed using DeltaGraph Pro (DeltaPoint Inc., version 4.0.1) for the Macintosh. Dose−response data were fit to a one-site stimulation model to obtain S_{max} and EC_{50} values. Saturation binding data were fit to a one-site binding model for B_{max} and K_d values. Ligand inhibition binding data were fit to one-site, two-site, and three-site binding models. Statistical comparisons between one-site and multiple-site models were carried out using an F test with a set at the 0.05 level. K_i values were converted from IC_{50} values according to the Cheng−Prusoff formula.[32] Analyses of variance with posthoc Tukey−Kramer tests were utilized for comparing differences in receptor binding affinity and receptor activation.

Molecular Modeling. The present M_1 muscarinic receptor model was constructed on the basis of the recently determined rhodopsin structure[9] (Protein Data Bank code 1F88). The alignment was made such that the amino acid homology between the rhodopsin PWQ 34−36 and NPxxYxxxN 302−310 sequences, and the corresponding 22−24 and 414−422 residues for the M_1 receptor was preserved. The alignment ensured that the Cys435 residue in the M_1 receptor corresponded to a Cys residue in rhodopsin, which was acylated by a palmitoyl group. To maintain the Cys98−Cys178 disulfide bond and the above correspondence for M_1 receptors, three residues were inserted and one was deleted from the loop areas of the rhodopsin template. The third intracellular loop was deleted between Gln226 and Lys353 where CH_3CO and NH−CH_3 end groups were provided. All ionizable side chains were considered charged. The model was built using the Sybyl (version 6.6) software of Tripos,[24] as implemented on a Silicon Graphics Indigo^2 workstation. The energy of the receptor model was minimized using the Tripos force field and all-atom AMBER charges[33] until an energy gradient of 0.05 kcal/mol/Å was reached.

For the ligands, AM1 charges[34] were determined and used in gas-phase and aqueous solution molecular dynamics simulations. By use of the Tripos force field, the program provided estimates for the missing force field parameters including those for the 1,2,5-thiadiazole ring atoms. Input structures for in-solution simulations were obtained from 100 ps gas-phase molecular dynamics simulations. The nonbonded cutoff was set to 17−20 Å, and a distance-dependent dielectric function was used in order to consider the electrostatic repulsion between the two positively charged tertiary amine groups. In

NVT simulations at $T = 310$ K, the aqueous solution was modeled by a periodic box in a thermal bath with a thermal coupling parameter of 100 fs. The system comprised the dication ligand, two chloride counterions, and about 1240 TIP3P water molecules. The cutoff was set to 8 Å in order to keep the calculations tractable. The electrostatic interaction energy was calculated according to the Coulomb formula with a dielectric constant of 1. All single bonds were subject to the SHAKE constraint, and the time step was set to 2 fs. After equilibration of 130−200 ps, the internal geometric parameters were analyzed from a further 200 ps simulation.

The conformation obtained for ligand **11c** at the end of the aqueous solution simulation was used for docking in the M_1 receptor model (structure **I**). Upon a manual adjustment, the ligand was placed in the third extracellular loop area so that the cationic heads were at distances of 4−5 Å from the carboxylate oxygens of Asp393 and Glu397. By use of the DOCK procedure of Sybyl with flexible geometries for both elements, the energy of the dimer was minimized. For structure **II**, an extended **11c** conformation was generated and placed into the channel. In the present preliminary calculations, an energy gradient limit of 0.05 kcal mol^{-1} $Å^{-1}$ was accepted, but even at this calculation level, the binding energy, EB = E(dimer) − E(receptor,opt) − E(ligand,opt), was about −30 to −40 kcal/mol, indicating favorable binding interactions at the selected sites.

Acknowledgment. The work was supported by Grants NS31173 and NS35127 from the National Institutes of Health and by a research contract from UCB Research, Inc. The authors thank Ms. Barbara Gardner and Ms. Sharon Troutman for their secretarial assistance in the preparation of the manuscript.

References

(1) Caulfield, M. P.; Birdsall, N. J. International Union of Pharmacology. XVII. Classification of muscarinic acetylcholine receptors. *Pharmacol. Rev.* **1998**, *50*, 279−290.
(2) Ellis, J. L.; Harman, D.; Gonzalez, J.; Spera, M. L.; Liu, R.; et al. Development of muscarinic analgesics derived from epibatidine: role of the M_4 receptor subtype. *J. Pharmacol. Exp. Ther.* **1999**, *288*, 1143−1150.
(3) Tecle, H.; Barrett, S. D.; Lauffer, D. J.; Augelli-Szafran, C.; Brann, M. R.; et al. Design and synthesis of m1-selective muscarinic agonists: (*R*)-(−)-(*Z*)-1-azabicyclo[2.2.1]heptan-3-one, *O*-(3-(3′-methoxyphenyl)-2-propynyl)oxime maleate (CI-1017), a functionally m1-selective muscarinic agonist. *J. Med. Chem.* **1998**, *41*, 2524−2536.
(4) Tecle, H.; Schwarz, R. D.; Barrett, S. D.; Callahan, M. J.; Caprathe, B. W.; et al. CI-1017, a functionally M_1-selective muscarinic agonist: design, synthesis, and preclinical pharmacology. *Pharm. Acta Helv.* **2000**, *74*, 141−148.
(5) Sauerberg, P.; Olesen, P. H.; Nielsen, S.; Treppendahl, S.; Sheardown, M. J.; et al. Novel functional M_1 selective muscarinic agonists. Synthesis and structure−activity relationships of 3-(1,2,5-thiadiazolyl)-1,2,5,6-tetrahydro-1-methylpyridines. *J. Med. Chem.* **1992**, *35*, 2274−2283.
(6) Sauerberg, P.; Olesen, P. H.; Sheardown, M. J.; Rimvall, K.; Thogersen, H.; et al. Conformationally constrained analogues of the muscarinic agonist 3-(4-(methylthio)-1,2,5-thiadiazol-3-yl)-1,2,5,6-tetrahydro-1-methylpyr idine. Synthesis, receptor affinity, and antinociceptive activity. *J. Med. Chem.* **1998**, *41*, 109−116.
(7) Portoghese, P. S.; Nagase, H.; Takemori, A. E. Only one pharmacophore is required for the κ opioid antagonist selectivity of norbinaltorphimine. *J. Med. Chem.* **1988**, *31*, 1344−1347.
(8) Takemori, A. E.; Ho, B. Y.; Naeseth, J. S.; Portoghese, P. S. Norbinaltorphimine, a highly selective kappa-opioid antagonist in analgesic and receptor binding assays. *J. Pharmacol. Exp. Ther.* **1988**, *246*, 255−258.
(9) Palczewski, K.; Kumasaka, T.; Hori, T.; Behnke, C. A.; Motoshima, H.; et al. Crystal structure of rhodopsin: A G protein-coupled receptor. *Science* **2000**, *289*, 739−745.
(10) Fraser, C. M.; Wang, C. D.; Robinson, D. A.; Gocayne, J. D.; Venter, J. C. Site-directed mutagenesis of m1 muscarinic acetylcholine receptors: conserved aspartic acids play important roles in receptor function. *Mol. Pharmacol.* **1989**, *36*, 840−847.
(11) Wess, J.; Gdula, D.; Brann, M. R. Site-directed mutagenesis of the m3 muscarinic receptor: identification of a series of threonine and tyrosine residues involved in agonist but not antagonist binding. *EMBO J.* **1991**, *10*, 3729−3734.
(12) Wess, J.; Maggio, R.; Palmer, J. R.; Vogel, Z. Role of conserved threonine and tyrosine residues in acetylcholine binding and muscarinic receptor activation. A study with m3 muscarinic receptor point mutants. *J. Biol. Chem.* **1992**, *267*, 19313−19319.
(13) Bluml, K.; Mutschler, E.; Wess, J. Functional role in ligand binding and receptor activation of an asparagine residue present in the sixth transmembrane domain of all muscarinic acetylcholine receptors. *J. Biol. Chem.* **1994**, *269*, 18870−18876.
(14) Bluml, K.; Mutschler, E.; Wess, J. Identification of an intracellular tyrosine residue critical for muscarinic receptor-mediated stimulation of phosphatidylinositol hydrolysis. *J. Biol. Chem.* **1994**, *269*, 402−405.
(15) Fanelli, F.; Menziani, M. C.; Carotti, A.; De Benedetti, P. G. Theoretical quantitative structure−activity relationship analysis on three dimensional models of ligand−m1 muscarinic receptor complexes. *Bioorg. Med. Chem.* **1994**, *2*, 195−211.
(16) Nordvall, G.; Hacksell, U. Binding-site modeling of the muscarinic m1 receptor: a combination of homology-based and indirect approaches. *J. Med. Chem.* **1993**, *36*, 967−976.
(17) Ward, S. D.; Curtis, C. A.; Hulme, E. C. Alanine-scanning mutagenesis of transmembrane domain 6 of the M_1 muscarinic acetylcholine receptor suggests that Tyr381 plays key roles in receptor function. *Mol. Pharmacol.* **1999**, *56*, 1031−1041.
(18) Huang, X. P.; Nagy, P. I.; Williams, F. E.; Peseckis, S. M.; Messer, W. S., Jr. Roles of threonine 192 and asparagine 382 in agonist and antagonist interactions with M_1 muscarinic receptors. *Br. J. Pharmacol.* **1999**, *126*, 735−745.
(19) Spalding, T. A.; Burstein, E. S.; Brauner-Osborne, H.; Hill-Eubanks, D.; Brann, M. R. Pharmacology of a constitutively active muscarinic receptor generated by random mutagenesis. *J. Pharmacol. Exp. Ther.* **1995**, *275*, 1274−1279.
(20) Spalding, T. A.; Burstein, E. S.; Wells, J. W.; Brann, M. R. Constitutive activation of the m5 muscarinic receptor by a series of mutations at the extracellular end of transmembrane 6. *Biochemistry* **1997**, *36*, 10109−10116.
(21) Spalding, T. A.; Burstein, E. S.; Henderson, S. C.; Ducote, K. R.; Brann, M. R. Identification of a ligand-dependent switch within a muscarinic receptor. *J. Biol. Chem.* **1998**, *273*, 21563−21568.
(22) Huang, X. P.; Williams, F. E.; Peseckis, S. M.; Messer, W. S., Jr. Pharmacological characterization of human m1 muscarinic acetylcholine receptors with double mutations at the junction of TM VI and the third extracellular domain. *J. Pharmacol. Exp. Ther.* **1998**, *286*, 1129−1139.
(23) Huang, X. P.; Williams, F. E.; Peseckis, S. M.; Messer, W. S., Jr. Differential modulation of agonist potency and receptor coupling by mutations of Ser388Tyr and Thr389Pro at the junction of transmembrane domain VI and the third extracellular loop of human M_1 muscarinic acetylcholine receptors. *Mol. Pharmacol.* **1999**, *56*, 775−783.
(24) *Sybyl*, version 6.6; Tripos, Inc.: St. Louis, MO, 1999.
(25) Jones, R. M.; Hjorth, S. A.; Schwartz, T. W.; Portoghese, P. S. Mutational evidence for a common kappa antagonist binding pocket in the wild-type κ and mutant μ[K303E] opioid receptors. *J. Med. Chem.* **1998**, *41*, 4911−4914.
(26) Messer, W. S., Jr.; Abuh, Y. F.; Ryan, K.; Shepherd, M. A.; Schroeder, M.; et al. Tetrahydropyrimidine derivatives display functional selectivity for M_1 muscarinic receptors in brain. *Drug Dev. Res.* **1997**, *40*, 171−184.
(27) Messer, W. S., Jr.; Abuh, Y. F.; Liu, Y.; Periyasamy, S.; Ngur, D. O.; et al. Synthesis and biological characterization of 1,4,5,6-tetrahydropyrimidine and 2-amino-3,4,5,6-tetrahydropyridine derivatives as selective m1 agonists. *J. Med. Chem.* **1997**, *40*, 1230−1246.
(28) Bonner, T. I.; Buckley, N. J.; Young, A. C.; Brann, M. R. Identification of a family of muscarinic acetylcholine receptor genes. *Science* **1987**, *237*, 527−532.
(29) Bonner, T. I.; Young, A. C.; Brann, M. R.; Buckley, N. J. Cloning and expression of the human and rat m5 muscarinic acetylcholine receptor genes. *Neuron* **1988**, *1*, 403−410.
(30) Dorje, F.; Wess, J.; Lambrecht, G.; Tacke, R.; Mutschler, E.; et al. Antagonist binding profiles of five cloned human muscarinic receptor subtypes. *J. Pharmacol. Exp. Ther.* **1991**, *256*, 727−733.
(31) Jones, S. V.; Choi, O. H.; Beaven, M. A. Carbachol induces secretion in a mast cell line (RBL-2H3) transfected with the ml muscarinic receptor gene. *FEBS Lett.* **1991**, *289*, 47−50.
(32) Cheng, Y.; Prusoff, W. H. Relationship between the inhibition constant (K_I) and the concentration of inhibitor which causes 50% inhibition (I_{50}) of an enzymatic reaction. *Biochem. Pharmacol.* **1973**, *22*, 3099−3108.
(33) Weiner, S. J.; Kollman, P. A.; Nguyen, D. T.; Case, D. A. An all atom force field for simulations of proteins and nucleic acids. *J. Comput. Chem.* **1986**, *7*, 230−252.
(34) Dewar, M. J. S.; Zoebisch, E. G.; Healy, E. F.; Stewart, J. J. P. AM1: A new general purpose quantum mechanical molecular model. *J. Am. Chem. Soc.* **1985**, *107*, 3902−3909.

JM0102405